Distribution Agreement

In presenting this thesis or dissertation as a partial fulfillment of the requirements for an advanced degree from Emory University, I hereby grant to Emory University and its agents the non-exclusive license to archive, make accessible, and display my thesis or dissertation in whole or in part in all forms of media, now or hereafter known, including display on the world wide web. I understand that I may select some access restrictions as part of the online submission of this thesis or dissertation. I retain all ownership rights to the copyright of the thesis or dissertation. I also retain the right to use in future works (such as articles or books) all or part of this thesis or dissertation.

Signature:

_____ _____

Kristina Dahlgren 7/10/2018

Investigating Functional Connectivity of the Amygdala
as a Function of Valence and Subsequent Memory

By

Kristina Dahlgren
B.S. Colorado State University, 2016
Psychology

_____
Stephan Hamann Ph.D.
Advisor

_____
Joseph. R. Manns Ph.D.
Committee Member

_____
Patricia A. Brennan Ph.D.
Committee Member

Accepted:

_____
Lisa A. Tedesco, Ph.D.
Dean of the James T. Laney School of Graduate Studies

_____
Date

Investigating Functional Connectivity of the Amygdala as a Function of Valence and Subsequent Memory

By

Kristina Dahlgren
B.S., Colorado State University, 2016

Advisor: Stephan Hamann, Ph.D.

An abstract of a thesis submitted to the Faculty of the
James T. Laney School of Graduate Studies of Emory University
in partial fulfillment of the requirements for the degree of Master of Arts
in Psychology
2018

Abstract

Investigating Functional Connectivity of the Amygdala
as a Function of Valence and Subsequent Memory
By Kristina Dahlgren

The amygdala has been shown to support emotional processing and emotional memory enhancement. Neuroimaging studies investigating the emotional enhancement of memory have found reliable activation in the amygdala as well as the prefrontal cortex, ventral visual stream, and the hippocampus. A remaining question is whether the prefrontal cortex, ventral visual stream, and hippocampus are interacting directly with the amygdala or whether they are operating independently of the amygdala. Recently, functional connectivity has been used to assess the degree to which these regions are interacting with the amygdala. However, few studies have analyzed functional connectivity for positive stimuli or functional connectivity between the amygdala and the whole brain. To investigate how regional activations and functional connectivity between the amygdala and the whole brain differ as a function of valence, this study examined emotional processing of and subsequent memory for positive, negative, and neutral pictures using a combined univariate analysis and beta series functional connectivity analysis. Widespread functional connectivity was observed between the amygdala and the hippocampus, prefrontal cortex, ventral visual stream, frontal lobe, parietal lobe, temporal lobe, subcortical structures, and cerebellum for positive, negative, and neutral pictures. Despite predictions, no significant differences in functional connectivity between the amygdala and any other brain regions were observed as either a function of valence or subsequent memory. As expected, increased amygdala activation was observed for both positive and negative subsequently remembered pictures compared to neutral pictures. Further, increased activation was also observed in the left hippocampus for subsequently remembered positive pictures, and for all positive, negative, and neutral pictures that were subsequently remembered combined. Taken together, these results do not show differences in functional connectivity between the amygdala and the hippocampus, prefrontal cortex, or visual processing regions during successful encoding of emotional information as a function of valence; nor do they replicate previous findings of increased functional connectivity between the amygdala and the hippocampus, prefrontal cortex, and visual processing regions during successful encoding of emotional information. Further research is needed to delineate how functional connectivity during the emotional enhancement of memory may differ as a function of valence.

Investigating Functional Connectivity of the Amygdala as a Function of Valence and Subsequent Memory

By

Kristina Dahlgren
B.S., Colorado State University, 2016

Advisor: Stephan Hamann, Ph.D.

A thesis submitted to the Faculty of the
James T. Laney School of Graduate Studies of Emory University
in partial fulfillment of the requirements for the degree of Master of Arts
in Psychology
2018

Table of Contents

Memory for emotional events are more accurate, more vivid, and longer lasting than neutral events (Cahill, 1997; Reisberg & Heuer, 2004). This emotional enhancement of memory is thought to be adaptive; however, in some cases this emotional enhancement of memory can become maladaptive and develop into memory related disorders for emotional events such as PTSD (Cahill, 1997). Thus, a major focus of current research seeks to understand how the brain processes and remembers emotional information. Understanding the neural underpinnings of the normal emotional memory enhancement effect can provide insight into how these processes can be altered to become maladaptive.

Role of the Amygdala in the Emotional Enhancement of Memory

Considerable evidence shows that the amygdala plays a critical modulatory role in emotional processing and emotional memory enhancement. Through direct and indirect pathways with multiple brain regions, the amygdala has been hypothesized to modulate attention, perception, and memory for emotional information (Phelps, 2004; Phelps & LeDoux, 2005; Vuilleumier, 2005). Nonhuman primate studies have shown that the amygdala has extensive direct structural projections to sensory processing cortices including all areas of the ventral visual stream (Amaral, Behniea, & Kelly, 2003), the auditory cortex (Yukie, 2002), somatosensory cortices via the insula (Friedman, Murray, O'Neill, & Mishkin, 1986), as well as the prefrontal cortex (Aggleton, Wright, Rosene, & Saunders, 2015), and the medial temporal lobe (MTL) memory system (Aggleton,1986). The MTL memory system is crucial to the development of long term declarative memory and includes the hippocampus, perirhinal cortex, and entorhinal cortex (Squire & Zola-Morgan, 1991). In addition to these direct pathways, hormones released by the adrenal cortex (epinephrine and cortisol) during emotional arousal influence the amygdala to indirectly modulate memory consolidation in the hippocampus and

other brain structures including the MTL memory system, and dorsal and ventral striatum (McGaugh, 2000; McGaugh, 2004; McGaugh & Roozendaal, 2002). It is through these direct and indirect pathways that the amygdala is thought to upregulate activity in other brain regions to enhance attention, perception, and memory for emotionally salient stimuli.

The role of the amygdala in modulating the emotional enhancement of perceptual processing (Anderson & Phelps 2001; Edmiston et al., 2013; Piech et al., 2011) and memory (Adolphs, Cahill, Schul, & Babinsky, 1997; Adolphs, Tranel, & Buchanan, 2005; Brierley, Medford, Shaw, and David, 2004; Cahill, Babinsky, Markowitsch, & McGaugh,1995; Phelps et al., 1998) has been examined in humans using studies of individuals with amygdala lesions. Some early amygdala lesion studies found that patients with selective bilateral amygdala lesions did not exhibit the normal memory enhancement effect for emotional pictures and stories (Adolphs, Cahill, Schul, & Babinsky, 1997; Cahill, Babinsky, Markowitsch, & McGaugh,1995); this finding seems to support the critical role of the amygdala in enhancing memory for emotional material. However, another study with patients with bilateral amygdala lesions found impaired fear conditioning but enhanced memory similar to controls for emotionally valanced words (Phelps et al., 1998) suggesting that the amygdala may be necessary for emotional enhancement of memory for some types of stimuli but not others.

In a more recent study, Brierley et al. (2004) found enhanced memory for emotional stories for some patients with amygdala lesions while others were severely impaired. Another study conducted by Adolphs et al. (2005) found that patients with amygdala lesions had decreased gist memory, memory for essential information necessary to understand the meaning of the picture as opposed to specific, detailed information, for emotional but not neutral pictures and that the extent of the impairment correlated with the extent of amygdala damage. Taken together, these

more recent findings from studies of patients with amygdala lesions suggest that amygdala lesions typically result in an impairment of the normal enhancement of memory for emotional material; however, in some cases normal emotional memory enhancement remains. Thus, the extent to which the amygdala plays a modulatory role in the emotional enhancement of memory remains unclear.

Neuroimaging of Emotional Memory Enhancement

In recent decades, functional neuroimaging methods have been increasingly used to noninvasively study the neural mechanisms of encoding and retrieval of emotional memory. Increased amygdala activity at encoding has been shown to be correlated with enhanced memory for emotional stimuli (both positive and negative) but not neutral stimuli (Canli, Zhao, Desmond, Glover, & Gabrieli, 1999; Hamann, Ely, Grafton, & Kilts, 1999; Kensinger & Schacter, 2006; Murty, Ritchey, Adcock, & LaBar, 2010) again stressing the importance of the amygdala in the emotional enhancement of memory. Additionally, these findings of increased amygdala activity during encoding for both positive and negative stimuli that are later remembered are consistent with the proposal that the involvement of the amygdala in emotional memory enhancement is driven primarily by arousal rather than valence (Davis & Whalen, 2001; Gläscher & Adolphs, 2003; Hamann, 2001; Hamann et al, 1999; Kensinger and Corkin, 2004).

However, during a shallow encoding task, Ritchey, LaBar, and Cabeza (2011) also found greater activation in the amygdala for subsequently remembered negative stimuli compared to positive stimuli. Additionally, Canli et al. (1999) found that while the amygdala responded with increased activation to subsequently remembered positive and negative stimuli compared to neutral stimuli; this response was greater for subsequently remembered negative stimuli than

positive stimuli. These two findings by Ritchey et al., and Canli et al., suggest that while the amygdala responds to arousal it may also respond differentially to valence.

Importantly, the amygdala does not function in isolation to achieve the emotional memory enhancement effect. In addition to the amygdala, other brain regions have also been shown to be active during encoding of emotional material that is later remembered. A recent metanalysis of neuroimaging studies identified regional activations for emotional items that were subsequently remembered compared to those that were forgotten (Murty et al., 2010). Results from this metanalysis were collapsed across valence (positive and negative stimuli combined) and were largely consistent with regions that have been identified in nonhuman primates as having direct structural projections from the amygdala including the MTL memory system (hippocampus, entorhinal cortex, perirhinal cortex, and parahippocampus), the ventral visual stream (middle temporal gyrus, middle occipital gyrus, fusiform gyrus), and prefrontal cortex (middle frontal gyri, and inferior frontal gyri). Findings of regional coactivations (increased activation for multiple brain regions at the same time during a cognitive task) during the emotional enhancement of memory in the amygdala, MTL memory system, ventral visual stream, and prefrontal cortex would be expected based on the hypothesis that the amygdala is directly modulating activity in these regions to enhance processing and memory for emotional events.

While the emotional enhancement effect has been shown for both positive and negative emotional stimuli, most neuroimaging studies using subsequent memory have primarily assessed the response to negative stimuli rather than positive stimuli. Or, similarly to the metanalysis mentioned above, studies examining the emotional enhancement of memory collapsed their results across valence (Murty et al., 2010). However, neuroimaging findings from studies that

examined differences in the way the brain processes positive and negative stimuli have led to several theories regarding how the brain may differentially support the emotional enhancement of memory depending on valence.

One hypothesis that has been advanced about how the brain might differentially process subsequently remembered positive and negative stimuli is that during encoding negative stimuli recruit greater visual processing; whereas positive stimuli recruit greater semantic processing (Kensinger & Schacter, 2008; Mickley & Kensinger, 2008). Another way in which the brain may differentially process subsequently remembered positive and negative stimuli is that processing may occur in different areas within the prefrontal cortex depending on valence. Specifically, activations in the lateral and medial prefrontal cortex may differ depending on valence (Dolcos, Labar and Cabeza, 2004a; Kensinger & Corkin, 2004; Kensinger & Schacter, 2006). A third possible explanation for how the brain may differentially process and remember emotional stimuli is that positive stimuli recruit greater processing in reward regions than negative and neutral stimuli. And finally, subsequently remembered positive stimuli may also recruit greater processing in regions associated with attention, visuospatial navigation, and target selection than negative stimuli.

Hamann et al. (1999) found greater activation for two regions in visual cortex and one region (not specified) in the frontal lobe for subsequently remembered positive stimuli compared to subsequently remembered neutral stimuli; while, subsequently remembered negative stimuli compared to neutral stimuli showed increased activation in one region of visual cortex and one region in the medial temporal lobe. Inconsistent with the perceptual vs semantic processing hypothesis, these findings suggest enhanced perceptual processing as well as enhanced semantic processing for both positive and negative subsequently remembered stimuli. Additionally, when

activity correlating with memory for positive stimuli was compared to neutral stimuli, Hamann et al. (1999) found greater activation the following medial prefrontal cortex regions associated with reward processing, the nucleus accumbens (Knutson, Adams, Fong, & Hommer, 2001), and anterior cingulate cortex (Bush et al., 2002) supporting the proposal that positive stimuli recruit enhanced reward processing and that activation in the prefrontal cortex differs as a function of valence.

Canli et al. (1999) found greater activation for subsequently remembered negative compared to positive pictures in the lateral prefrontal cortex (right middle frontal gyrus, left inferior frontal gyrus) as well as the left precentral gyrus, left superior temporal gyrus, and bilateral insula; and for subsequently remembered positive pictures compared to negative pictures increased activation was observed in the medial prefrontal cortex (left anterior cingulate). These findings of enhanced processing in the temporal lobe for subsequently remembered negative pictures, and enhanced processing in reward associated anterior cingulate (Bush et al., 2002) for subsequently remembered positive stimuli, do not support the perceptual vs semantic processing hypothesis. Instead, these findings suggest enhanced semantic processing for both positive and negative stimuli. However, they do support the findings of differential activation in the prefrontal cortex as a function of valence.

Ritchey et al. (2011) found greater activation for subsequently remembered positive compared to negative stimuli in both lateral and medial prefrontal cortex (superior frontal gyrus and middle frontal gyrus), visual processing regions (cuneus and lingual gyrus), and the parietal lobe (precuneus); suggesting both enhanced perceptual and semantic processing for positive stimuli compared to negative stimuli as well as differential valence effects in the prefrontal cortex. Further, greater activation for positive compared to negative stimuli was found in the

reward implicated caudate nucleus (Balleine, Delgado, & Hikosaka, 2007). Additionally, differential activation was observed in areas associated with attention, visuospatial navigation, and target selection for positive subsequently remembered stimuli compared to negative stimuli. Ritchey et al. found greater activation for positive compared to negative stimuli in the retrosplenial cortex which has been associated with navigation and scene processing (Maguire, 2001; Epstein, 2008), and the precuneus which has been associated with directing attention, visuospatial mental operations, and self-referential processing (Cavanna & Trimble, 2006). Moreover, greater activation was observed for positive compared to negative stimuli in the superior colliculus which is involved in controlling gaze (Sparks, 1999), multisensory integration (Alais, Newell, & Mamassian, 2010), visuospatial attention (Krauzlis, Lovejoy, & Zénon, 2013), and target selection (Krauzlis, Liston, & Carello, 2004), when deep encoding was used rather than shallow encoding.

In summary, it has been suggested that during the emotional enhancement of memory positive stimuli recruit greater semantic processing while negative stimuli recruit greater perceptual processing. Neuroimaging findings based on coactivations have shown that subsequently remembered positive stimuli seem to elicit greater activation in areas associated with reward (Canli et al., 1999; Hamann et al., 1999; Ritchey et al., 2011), attention, visuo-spatial, and self-referential processing regions (Ritchey et al., 2011) compared to negative and neutral stimuli. These findings are compatible with the suggestion that subsequently remembered positive stimuli recruit greater semantic processing than negative stimuli and provide additional details about the types of semantic processing that might be recruited. However, greater activations for negative stimuli in the temporal lobe (Canli et al., 1999; Hamann et al 1999) suggest enhanced semantic processing for negative stimuli as well. Regarding the proposal that

negative stimuli recruit enhanced visual processing compared to positive stimuli, neuroimaging activation results have shown enhanced processing for both positive (Hamann et al., 1999; Ritchey et al., 2011) and negative stimuli (Hamann et al.,1999) in areas in the ventral visual stream suggesting enhanced perceptual processing is recruited for both positive and negative visual stimuli. As for the proposal that valence may differentially recruit processing in different areas of prefrontal cortex, negative remembered stimuli tend to elicit increased activation in lateral prefrontal cortex (Canli et al., 1999; Hamann et al., 1999; Kensinger & Corkin, 2004; Kensinger & Schacter, 2006) while positive remembered stimuli tend to elicit increased activation in the medial prefrontal cortex (Canli et al., 1999; Hamann et al., 1999; Kensinger & Schacter, 2006); however, other studies found increased activations in both lateral and medial prefrontal cortex for positive stimuli (Dolcos et al, 2004a; Ritchey et al., 2011). Thus, it remains unclear how the brain differentially processes and remembers emotional information as a function of valence.

Functional Connectivity and Emotional Memory Enhancement

Complex cognitive processes such as emotion processing and memory formation require interaction between multiple brain regions operating in concert to form networks (Sporns, Chialvo, Kaiser, & Hilgetag, 2004; Sporns, 2013; Hermundstad et al., 2013). Inferences regarding how the brain processes and remembers emotional information have primarily been made based on neuroimaging studies that have examined brain regions that are differentially active during encoding of emotional stimuli. However, the fact that two regions are active at the same point in time during a cognitive task does not constitute sufficient evidence that these regions are functionally interacting. Functional connectivity analysis is a powerful technique that examines correlated brain activity across multiple brain regions over multiple time points to

determine how brain regions interact to form networks (Friston, Buechel, Fink, Morris, Rolls, & Dolan, 1997; Van Den Heuvel, & Pol, 2010).

To date, relatively few studies have used functional connectivity analyses to examine the effects of valence on emotional memory. Therefore, using functional connectivity to examine the interaction between brain regions may be a useful method to further elucidate the effects of valence on emotional memory enhancement. In a review of brain imaging studies that looked at the neural correlates of emotional memory, Dolcos, Denkova, and Dolcos, (2012) suggested that the effects of valence may be found in connections between brain regions and involve regions outside the MTL. Moreover, in a study using functional connectivity to look at the neural correlates of emotional memory, Ritchey et al. (2011) suggested that the interaction between amygdala and the MTL may depend on valence.

Functional connectivity has been used in many ways to study the interactions between brain regions. One way in which functional connectivity is studied is through resting state functional magnetic resonance imaging (Van Den Heuvel, & Pol, 2010). Resting state functional connectivity studies examine how brain regions are interacting when the brain is not performing any specific cognitive tasks, instead participants are instructed to relax and not think about anything in particular (Van Den Heuvel, & Pol, 2010). While this type of functional connectivity analysis can be useful for understanding differences in baseline network connectivity (Van Den Heuvel, & Pol, 2010), it does not provide information on how emotional information is processed and remembered because it is often unknown exactly what participants are thinking about during these rest periods. Moreover, there is substantial individual variability in subjective experiences during resting state scans (Hurlburt, Alderson-Day, Fernyhough, & Kühn, 2015). Thus, to address the question of how the brain is functionally connected during

emotional memory processing, a task based functional connectivity analysis in which participants are performing an emotional memory task is necessary to make these distinctions.

Several methods of conducting task based functional connectivity analyses have been used to examine the emotional memory enhancement effect. The simplest method for measuring functional connectivity is to examine correlations between the time course of activity in one brain region and activity in another brain region (Friston et al., 1997). However, this method is limited to investigating direct interaction between only two regions at a time such that multiple correlations must be calculated to examine interactions between more than two regions. Furthermore, it is possible that correlations of regional activations observed in this manner may be a result of modulation of both regions by a third region.

Another functional connectivity method, psychophysiological interactions (PPI), uses linear regression analyses in which activity in one or more brain regions are regressed onto activity for another brain region during different conditions (Friston et al.1997). The extent to which the slope of the regressions changes is an indicator of how one or more regions may be influencing each other. One strength of the PPI method is that it allows for inferences regarding directionality to be made (Friston et al., 1997). Another strength of the method is that interactions between multiple brain regions can be examined in the same analysis and can help to resolve the issue of whether an interaction between two regions is being driven by a third region. One limitation of this method is that it is still limited to a few regions of interest determined *a priori* and doesn't provide information about how a region may be interacting with the whole brain. Another limitation of this method is that only the mean values for each condition are correlated such that it examines overall activity during a condition but does not consider trial by trial variability.

A third functional connectivity analysis method, structural equation modeling, primarily uses a small fixed network of a few brain regions and allows for inferences regarding directionality (Zhuang, Peltier, He, LaConte, & Hu, 2008). Structural equation modeling can be used to create a model of a few fixed brain regions and allows for the strength of connections to be assessed going both to and from multiple regions of interest. However, this method still does not allow for examination of interactions between one region and the whole brain. A fourth functional connectivity analysis method, beta series correlation, uses a seed region or seed voxel and examines correlations between activity in the seed region or voxel and activity in all other voxels in the brain for all events within a condition rather than averaging across events within a condition (Rissman, Gazzaley, & D'esposito, 2004).

The simple regression method was used by Dolcos, Labar, and Cabeza (2004b) to show that activity between the amygdala, hippocampus, and entorhinal cortex were more highly correlated for emotional items that were remembered compared to forgotten than for neutral items that were remembered compared to forgotten. This finding suggests that the amygdala and medial temporal lobe memory system (MTL memory system) interact to enhance memory for emotional stimuli but not neutral stimuli. Because the analysis method used by Dolcos et al. (2004b) only examined interactions between pairs of brain regions, it provides an incomplete picture of how the amygdala may interact with other brain regions to facilitate the emotional enhancement of memory. Another limitation of this study is that it used an analysis method that collapsed across subsequently remembered positive and negative stimuli; thus, differential effects of valence could not be examined.

Ritchey et al. (2011) used PPI with a multiple regression analysis to examine how deep and shallow encoding instructions affected the emotional enhancement of memory for positive,

negative, and neutral pictures. By regressing anatomical regions of interest (ROIs) of the amygdala and right ventrolateral prefrontal cortex (vlPFC) on the hippocampus, Ritchey et al. sought to determine whether activity in the amygdala and/or vlPFC modulated activity in the hippocampus during the emotional enhancement of memory. Ritchey et al. found that memory for negative items were correlated with increased connectivity between the amygdala and hippocampus while memory for positive items were associated with increased connectivity between the hippocampus and prefrontal cortex. However, because this study only examined interactions between three ROIs this study does not provide a clear a picture on how these regions interact with other regions, such as visual processing regions, nor do they consider how these regions interact over time within a condition because they averaged across the condition when extracting regressors (Ritchey et al., 2011).

Mickley Steinmetz, Addis, and Kensinger (2010) used structural equation modeling to look at differences in functional connectivity between the left amygdala, left hippocampus, left inferior frontal gyrus, left middle occipital gyrus, and left fusiform gyrus for subsequently remembered positive arousing, positive non-arousing, negative arousing, and negative non-arousing pictures. Mickley et al. observed stronger connections for subsequently remembered negative arousing pictures compared to negative non-arousing pictures from the left amygdala to the left inferior frontal gyrus and left middle occipital gyrus as well as stronger connections between the fusiform and middle occipital gyrus. On the other hand, stronger connections were observed for subsequently remembered positive non-arousing pictures compared to positive arousing pictures from the amygdala to the inferior frontal gyrus, hippocampus, and middle occipital gyrus. While the design of this study allowed for directionality inferences, it was limited to a set number of regions within the left hemisphere; therefore, it is unclear if these same

patterns of connectivity would be observed in the right hemisphere or how additional regions, such as those associated with reward and visuospatial navigation, may be modulated during the emotional enhancement of memory.

St. Jacques, Dolcos, Cabeza (2009) used a beta series correlation approach with a seed voxel located in the amygdala to look at the effects of aging on functional connectivity for the emotional enhancement of subsequent memory between the amygdala and the whole brain. Age-related decreases in functional connectivity were found between the amygdala and hippocampus and VLPFC as well as increased functional connectivity between the amygdala and DLPFC, fusiform gyrus, posterior parietal cortex, and cerebellum for subsequently remembered negative stimuli compared to neutral stimuli (St. Jacques et al., 2009). Positive stimuli were excluded from analysis because many of the positive pictures presented contained erotic or radical sport content (St. Jacques et al., 2009) which may be processed differently in older adults compared to younger adults (Backs, da Silva, & Han, 2005). While this study allowed for the examination of age-related differences in functional connectivity between the amygdala and the entire brain for the emotional enhancement of memory, differences in connectivity were only analyzed for subsequently remembered negative stimuli compared to neutral stimuli even though positive stimuli were also presented (St. Jacques et al., 2009).

Ritchey, Dolcos, and Cabeza (2008) also used a beta series correlation approach to examine whole brain functional connectivity between a peak voxel in the left amygdala and the whole brain for subsequent memory of negative pictures over short (20 minutes) and long (1 week) delays. Increased functional connectivity was observed for subsequently remembered emotional compared to neutral items between the amygdala and parahippocampal cortex, and between the amygdala and parietal and medial frontal regions for long delays. On the other hand,

greater connectivity was observed between the amygdala and the medial frontal gyrus for short delays. While this study allowed for the examination of differences in functional connectivity between the amygdala and the whole brain for subsequently remembered emotional stimuli over short and long delays, this study only presented negative pictures preventing observation of differences in functional connectivity as a function of valence.

To date, these are the only studies to have examined the effects of valence on amygdala functional connectivity for the emotional enhancement of subsequent memory. Taken together, these studies are insufficient to determine how the amygdala interacts with the whole the brain during the emotional enhancement of memory for both positive and negative stimuli because they examined correlations between only a few specific brain regions (Dolcos et al., 2004b; Mickley Steinmetz et al, 2010; Ritchey et al, 2011;) collapsed across valence (Dolcos et al., 2004b), or only examined negative stimuli (Jacques et al 2009; Ritchey, et al 2008). The current study sought to understand how the brain differentially enhances processing of positive and negative pictures during the emotional enhancement of memory by investigating regional activations as well as functional connectivity between the amygdala and the whole brain to see how they differ as a function of valence and subsequent memory.

Current Study

The present study had three main goals. The first goal was to understand how the amygdala interacts with the MTL memory system, ventral visual stream, and prefrontal cortex to support the emotional enhancement of memory. The second goal was to determine what additional brain regions the amygdala may interact with to support the emotional enhancement of memory. The third goal was to determine how the amygdala may differentially interact with other brain regions during the emotional enhancement of memory based on the valence of the stimuli.

To better understand the amygdala's role in enhancing processing and memory for emotional events, the present paper investigated interactions between the amygdala and the MTL memory system, ventral visual stream, and prefrontal cortex. The amygdala, MTL memory system, ventral visual stream, and prefrontal cortex are brain regions that are reliably coactivated during presentation and subsequent memory for both positive and negative stimuli compared to neutral stimuli (Murty et al., 2010); therefore, enhanced regional activations in these regions were expected for both positive and negative remembered items compared to neutral remembered items. Because the amygdala modulation hypothesis suggests that the amygdala directly modulates activity in the MTL memory system, including the hippocampus, during the emotional enhancement of memory (McGaugh, 2004; Phelps, 2004), enhanced functional connectivity between the amygdala and MTL memory system was expected for both positive and negative remembered items compared to neutral remembered items. However, little is known regarding how the amygdala differentially interacts with the MTL memory system, visual ventral stream, and prefrontal cortex during the emotional enhancement of memory as a function of valence; therefore, the following whole brain functional connectivity predictions were exploratory in nature. Enhanced functional connectivity between the amygdala, MTL memory system, the ventral visual stream, and/or the prefrontal cortex, for emotional remembered items that are either positive or negative would suggest that the interaction between with these regions and the amygdala recruits additional cognitive processing to support the emotional enhancement of memory regardless of valence. Alternatively, during the emotional enhancement of memory, the amygdala might flexibly recruit additional processing in the MTL memory system, ventral visual stream, and/or prefrontal cortex based on the valence of the stimuli.

While investigating how the amygdala interacts with the MTL memory system, ventral visual stream, and prefrontal cortex is necessary to understand how the brain supports the emotional enhancement of memory, a more complete understanding requires examination of how the amygdala interacts with other brain regions as well. Additional brain regions that might be interacting with the amygdala to support the emotional enhancement of memory include reward processing regions, visuospatial processing regions, and regions involved in navigation. Enhanced functional connectivity for subsequently remembered emotional stimuli compared to neutral stimuli between the amygdala and brain regions involved in reward or visuospatial processing would suggest that recruitment of additional cognitive processing aids in the emotional enhancement of memory. For example, enhanced functional connectivity for positive but not negative or neutral subsequently remembered stimuli between the amygdala and regions such as the nucleus accumbens, caudate nucleus, and ACC would suggest that additional reward processing may help facilitate the emotional enhancement of positive memory. Similarly, enhanced connectivity for positive subsequently remembered stimuli, but not negative or neutral stimuli, between the amygdala and regions such as the precuneus and retrosplenial cortex suggests that the recruitment of visuospatial and navigation processes may assist with successful emotional memory encoding for positive stimuli.

To address these questions, this study used beta series correlation functional connectivity analyses, which are especially suited to event related designs compared to other methods of assessing functional connectivity (Rissman, Gazzaley, & D'esposito, 2004), to examine how interactions between the amygdala and the rest of the brain during the emotional enhancement of memory are affected by valence. Left and right amygdala seed regions were selected to compare functional connectivity between the amygdala and the whole brain during encoding of positive,

negative, and neutral pictures. Additionally, small volume correction (SVC) analyses were conducted on univariate regional activations and functional connectivity results with bilateral hippocampal and amygdala masks. To study differential activations and connectivity as a function of valence and memory, presented stimuli were later tagged as remembered or forgotten based on a memory test that occurred outside the scanner; this procedure is known as a subsequent memory paradigm (Paller & Wagner, 2002).

Methods

Subjects

18 right handed subjects (13 female) were recruited from the local community via advertisements. All subjects were screened to confirm they were not taking psychotropic medication and had no history of neurological or psychiatric impairment. The current study was part of a larger study focusing on sex differences in emotion processing and responses to sexual stimuli (for additional selection criteria associated with this larger study, see Hamann et al., 2014). The study was approved by the Institutional Review Boards of the participating universities. Of the initial subject pool, 5 males and 10 females were removed from final analyses due to either part of the brain being outside of the scanner field of view (1 male) or an insufficient number of trials for each condition (4 males and 10 females). Thus, the final analyses consisted of 10 males (mean age 27.2 years [SD = 4.24]) and 3 females (mean age 25.33 years [SD = 4.04]).

FMRI Scanning

Scanning was conducted using a 3 T Siemens Tim Trio MRI System and 12 channel parallel head coil. High resolution (1 x 1 x 1 mm) T1-weighted (MP-RAGE) images were collected for anatomical visualization. Functional data were acquired using a gradient-echo,

echoplanar pulse sequence (TR = 2000 ms, TE = 30 ms, Flip angle = 90 degrees, 37 horizontal interleaved slices, 3 x 3 x 3 mm voxel size). Each run contained 280 scan volumes.

Stimuli and Tasks

During scanning, subjects viewed positive, negative, and neutral stimuli selected from the IAPS picture database (Lang, Bradley, & Cuthbert, 1997). This database was used because normative ratings related to arousal and valence have been provided for each picture. Only valence ratings were used to determine whether a picture was positive, negative, or neutral. In addition, a small number of stimuli acquired from internet sources were also used for which normative ratings of arousal and valence were obtained in previous pilot sessions. These images were projected from a MacBook pro laptop running PsyScope (http://psy.ck.sissa.it/) (Cohen, J., MacWhinney, Flatt, & Provost, 1993) to subjects in the scanner via an LCD side-projection system and mirror. Subjects wore headphones to reduce scanner noise and were fitted with foam pads to reduce head motion.

Thirty-six images of each image type (positive, negative, and neutral) were presented pseudorandomly for 1.5 s each in one scanning run. Two additional buffer items were added (one each at the beginning and end of the run) to account for serial position effects and were modeled as error trials. During image presentation, subjects were instructed to view the images naturally and to experience any thoughts or feelings elicited by the images.

Following each image presentation, a response screen was presented for 1.5 s in which subjects were asked to rate whether they liked, disliked, or felt neutral towards the contents of the previous image. Subjects indicated their response (like, neutral, or dislike) by pressing the corresponding button on a scanner compatible fiber-optic button pad. Any item which was not rated was marked as an error trial. The ratings screen was followed by a pseudorandomly

alternating inter-trial fixation interval during which a white "+" on a black background was presented for either 1.5 or 2.5 seconds (Figure 1).

After completion of the scanning run, subjects' memory was tested using recall and recognition memory tests. A free recall task was conducted in the scanner during which subjects were asked to recall the descriptions of the previously presented pictures in any order. Next, a combined cued recall and recognition test was conducted out of the scanner approximately 15 to 30 minutes after completion of scanning. During the combined cued recall and recognition task subjects were read a phrase that corresponded to a picture that was either shown or not shown in the scanner. For example, the phrase "large statue" would be a cue for a picture of the statue of liberty at sunset. After hearing the cue, subjects were asked to decide if the picture had been presented. If the subject recognized the image they were asked to rate the vividness of their recall of the image on a scale of 1-5 (1 = not vivid at all, 3 = moderately vivid, 5 = very vivid) then they were asked to provide additional details about the picture so that cued recall of the memory could be verified; the subject could elect to pass if they did not recall the item. Finally, subjects were asked to rate how emotionally arousing the picture was (1 = very little or no emotional arousal, 3 = moderate emotional arousal, 5 = high emotional arousal). Statistical analyses were only performed on the cued recall task and on subjects who had a minimum of 8 trials of each type for the subsequent memory conditions.

Behavioral Analyses

Behavioral ratings were analyzed in SPSS24 using a two-factor within-subject repeated measures ANOVA with subject mean emotional arousal ratings as the dependent measure and valence (positive, negative, or neutral) and subsequent memory status (recalled or not recalled) as the repeated-measures factors.

FMRI Analyses

During preprocessing of functional images, differences in slice acquisition timing were corrected, images were realigned, estimated, and resliced using 5th degree B-spline interpolation; normalized to the standard Montreal Neurological Institute (MNI) anatomical template; and smoothed at 6 mm full-width half maximum (FWHM) using SPM 12 (http://www.fil.ion.ucl.ac.uk/spm/) (Friston et al, 1994). Next, motion correction was performed using independent component analysis (ICA) automatic removal of artifacts (ICA-AROMA). ICA based removal of motion artifacts identifies time-courses of independent components related to activity and noise and then regresses out components associated with noise. ICA-AROMA uses a classifier based on two temporal and two spatial features to automatically eliminate activity associated with head motion and performs as well or better than a 24 motion regressor, spike regressor, scrubbing, and other ICA motion correction options, while preserving the temporal characteristics of the fMRI data and limiting loss of degrees of freedom resulting in increased statistical power (Pruim, Mennes, Buitelaar, & Beckmann, 2015; Pruim et al, 2015). ICA-AROMA's non-aggressive de-noising option, which uses a partial component regression (Pruim, Mennes, van Rooij, et al., 2015), was selected for these analyses.

After preprocessing, two separate sets of statistical analyses were conducted including regional activation analyses and beta series functional connectivity analyses; SVC analyses were then performed on both the regional activations and functional connectivity results. Regional activations and functional connectivity were further analyzed using two separate models, one based only on the emotional valence of the presented images, and the other based on subsequent memory as a function of valence. The model that investigated differences in emotional valence consisted of three conditions corresponding to the positive, negative, and neutral images while

the model that examined differences in subsequent memory as a function of valence consisted of seven conditions corresponding to positive recalled images, positive not recalled images, negative recalled images, negative not recalled images, neutral recalled images, neutral not recalled images, and error trials (trials in which subjects did not make a response in the scanner).

Regional activations.

Regional activation analyses were conducted in SPM12. For individual subjects, brain activations for each condition were modeled with a train of delta functions representing the onset and duration, convolved with a canonical hemodynamic response function (HRF) with no temporal or dispersion derivatives, and filtered with a 128 HZ high pass filter to eliminate slow signal drift. Motion parameters were not included as regressors as motion correction was performed during preprocessing using ICA-AROMA. Activity was then masked using a brain mask that includes the entire brain but excludes the orbit which was created in MarsBaR (http://marsbar.sourceforge.net/) (Brett, Anton, Valabregue, & Poline, 2002) by thresholding a group averaged T1 subject image from SPM's canonical images and removing the eye region thereby restricting statistical comparisons to areas within the brain where brain activity would be expected, thus minimizing the number of comparisons being made and increasing degrees of freedom when controlling for false positives . The inter-trial fixation period served as an implicit baseline. Activation differences between conditions (e.g., positive stimuli vs. neutral stimuli) were assessed using linear contrast images for each subject with corresponding estimated beta-weights at every voxel in the brain.

Functional connectivity.

Functional connectivity analyses were performed using BASCO (BetA-Series COrrelation) (https://www.nitrc.org/projects/basco/) (Göttlich, Beyer, & Krämer, 2015) which

uses the beta series approach first described by Rissman, Gazzaley, and D'esposito (2004). Beta series analyses differ from standard univariate analyses in that they generate a parameter estimate or beta weight for each individual trial within each condition rather than averaging across trials to generate a single parameter estimate for each condition; this results in a series of parameter estimates or beta weights. Identifying and correlating activity on a trial by trial basis allows for a unique characterization of the functional connectivity between regions that is not obtainable via other functional connectivity methods that average across trials. Condition-specific Fisher z transformed correlation maps are then created by correlating the beta series for all voxels within a designated seed region, or seed voxel, with the beta series for all other voxels in the brain. Correlating the series of beta weights between one region, or voxel, and another provides information on how the activity of these brain regions or voxels correlate over time within a condition of interest resulting in a measure of functional connectivity. Once correlations between regions have been computed for each condition, these correlations can then be compared between conditions. Higher correlations are interpreted as greater functional connectivity between regions, or voxels, while lower correlations are interpreted as lower functional connectivity. Only positive correlations were examined.

Because the amygdala is critical for emotion processing and the emotional enhancement of memory (Phelps, 2004), the left and right amygdala were used as separate seed regions. Anatomical masks were created in MarsBaR based on the WFU Pickatlas (http://fmri.wfubmc.edu/software/PickAtlas) (Maldjian, Laurienti, & Burdette, 2003; Maldjian, Laurienti, & Burdette JH, 2004) implementation of the Automated Anatomical Labeling (AAL) (Tzourio-Mazoyer et al., 2002) parcellations for the entire left and right amygdala. Like the regional activations analyses, the time courses of predicted activity in the functional connectivity

analyses were convolved with a canonical HRF without derivatives or motion regressors and masked with an explicit brain mask excluding the orbit. Whole brain condition-specific functional correlation maps were generated as a function of valence, and as a function of subsequent memory and valence, for both the left and right amygdala seed regions. Additional correlation maps that combined conditions were generated as follows: positive and negative conditions were combined to create a condition that examined the general effect of emotion; and positive, negative, and neutral conditions were combined to create a condition that examined the effect of complex visual stimuli. Similarly, combined conditions were generated including: all recalled (positive recalled, negative recalled, and neutral recalled), all not recalled (positive not recalled, negative not recalled, and neutral not recalled); emotion recalled (positive recalled and negative recalled); emotion not recalled (positive not recalled and negative not recalled) and all visual (all positive, all negative, and all neutral).

To identify changes in functional connectivity as a function of valence and subsequent memory, these condition-specific and combined correlation maps were subtracted from each other using SPM12's Imcalc function. To identify functional connectivity changes as a function of memory, correlation maps for all not recalled items were subtracted from correlation maps for all recalled items. To identify changes in connectivity as a function of valence and subsequent memory, difference in memory correlation maps were calculated; all positive not recalled items were subtracted from all positive recalled items, and all negative not recalled items were subtracted from all negative recalled items, all emotional not recalled items were subtracted from all emotional recalled items, and all neutral not recalled items were subtracted from neutral recalled items. To identify functional connectivity associated with the emotional enhancement of

memory, the neutral difference in memory connectivity maps were subtracted from all the other emotional difference in memory connectivity maps.

Statistical significance for the functional connectivity correlation maps was assessed in SnPM13 (http://warwick.ac.uk/tenichols/snpm) by performing a one sample t-test on the Imcalc generated individual subject-specific contrast images. SnPM corrects for multiple comparisons using a cluster extent thresholding and nonparametric permutation testing approach based on locally pooled smoothed variance estimates and generates a pseudo-t statistic based on the smoothed variance estimates rather than a t-statistics based on the raw voxel-wise variance estimates; this method outperforms the general linear model when there are few degrees of freedom (Nichols & Holmes, 2001). Variance smoothing of 6 x6 x 6 mm FWHM was used and activity was masked using a 40 percent grey matter brain mask to restrict statistical calculations to brain regions where brain activation is expected, i.e. grey matter rather than white matter or cerebrospinal fluid, minimizing the number of comparisons being made and increasing degrees of freedom when controlling for false positives (Berns et al., 2012). 5000 permutations were performed with a cluster defining threshold of 3.01 corresponding to a voxel-wise threshold of $p<.001$ (Woo, Krishnan, & Wager, 2014), and a cluster threshold family wise error (FWE) rate was corrected to $p<.05$, resulting in separate critical supra-threshold cluster size (critical STCS) thresholds for each contrast.

Small volume correction.

Strong *a priori* evidence indicates that the amygdala is critical for emotion processing (Phelps, 2004). Similarly, the hippocampus is critical for successful declarative memory encoding (McGaugh, 2000). In addition, the amygdala modulation hypothesis suggests that the amygdala directly modulates activity in the hippocampus to enhance memory for emotional

information (McGaugh, 2004; Phelps, 2004). Because of the strong *a priori* functional hypotheses associated with the amygdala and hippocampus, SVC analyses (Poldrack, 2007) were performed for these regions. By restricting the analyses of functional connectivity between the amygdala seed region to a smaller spatial extent (i.e., number of voxels), SVC analyses reduce the number of statistical comparisons made and thereby increase the statistical power to detect significant effects in these regions. Statistical significance for the SVC analyses was assessed in SnPM13 with masks generated in MarsBaR based on WFU Pickatlas AAL parcellation using either a bilateral amygdala mask, a bilateral hippocampal mask, or both, depending on the specific analysis. Statistical significance was assessed using the same thresholds described previously in the functional connectivity analyses (5000 permutations, cluster defining single-voxel threshold of 3.01, and cluster threshold FWE rate of $p<.05$). To avoid conducting group-level analyses twice for the voxels in the SVC target regions (e.g., conducting successive t-tests for the whole-brain analysis and again for the separate SVC analysis in the voxels comprising the amygdala) and thereby inflating the group-level false positive rate for the SVC regions, the results of the whole brain analyses were omitted for voxels within the SVC regions, and the results of the SVC analysis were used instead. Thus, the whole-brain and SVC analyses were spatially complementary and nonoverlapping.

Because this study was specifically interested in differences in amygdala activation for emotional pictures compared to neutral pictures, SVC was only performed on the individual contrast-specific parametric activation maps with a bilateral amygdala mask for the contrasts that compared emotional and neutral conditions, namely, the negative>neutral, positive>neutral, and emotion>neutral contrasts. Similarly, this study was specifically interested in differences in amygdala and hippocampal activations for differences in memory as a function of valence.

Therefore, SVC analyses were performed on individual contrast-specific parametric maps with a bilateral amygdala mask and a bilateral hippocampal mask separately on the contrasts that examined subsequent memory as a function of valence, namely, the negativeDM>neutralDM**,** positiveDM>neutralDM**,** emotionDM>neutralDM**,** negativeDM**,** positiveDM**,** emotionDM**,** neutralDM contrasts. Only a hippocampal masked was used for the DM contrast as this contrast included all subsequently remembered stimuli regardless of valence.

Finally, this study was specifically interested in differences in functional connectivity between the amygdala and hippocampus for subsequently remembered emotional stimuli compared to neutral stimuli. Therefore, SVC analyses were performed on functional connectivity individual subject amygdala seed region contrast-specific correlational maps with a bilateral hippocampal mask only for the contrasts that examined subsequent memory as a function of valence, namely, the negativeDM>neutralDM, positiveDM>neutralDM**,** emotionDM>neutralDM**,** negativeDM**,** positiveDM**,** emotionDM, and neutralDM conditions.

Results

Behavioral Results

A valence (positive, negative, neutral) × memory (recalled, not recalled) ANOVA on arousal ratings revealed a significant effect of valence $F(2, 11) = 19.55$, $p < .001$, $\eta^2 = .962$, and memory $F(1, 12) = 17.8$, $p = .001$, $\eta^2 = .625$, but no interaction between valence and memory $F(1, 11) = 2.58$, $p = .121$, $\eta^2 = .134$ (Figure 4). Follow up Bonferroni-corrected pairwise comparisons for valence indicated that subjects rated both negative stimuli ($M = 3.29$, $SD = 0.87$) and positive stimuli ($M = 2.91$, $SD = 0.88$) as more arousing than neutral stimuli ($M = 1.85$, $SD = 0.60$) with $p = .002$ and $p < .001$ (Figure 2). Follow up Bonferroni-corrected pairwise comparisons for valence indicated that arousal ratings were significantly higher for the stimuli

that were recalled (M = 5.49, SD = 2.25) compared to the not recalled stimuli (M = 0.88, SD = 1.21) (Figure 3).

Neuroimaging Results

Functional connectivity.

First, to determine how the left and right amygdala seed regions interact with the whole brain while processing emotional and neutral visual stimuli, functional connectivity was calculated as a function of valence (positive, negative, neutral, emotion, all complex visual stimuli). Widespread functional connectivity was observed in several extensive clusters spanning multiple cortical brain regions (including the MTL memory system, prefrontal cortex, ventral visual stream cortex, frontal lobe, parietal lobe, temporal lobe) and subcortical brain regions including the contralateral amygdala, for all complex visual stimuli (positive, negative, and neutral combined [left amygdala seed Table 1; right amygdala seed Table 2]), all neutral stimuli (left amygdala seed Table 3, right amygdala seed Table 4), all emotional stimuli (positive and negative stimuli combined [left amygdala seed Table 5, right amygdala seed Table 6], negative stimuli (left amygdala seed Table 7, right amygdala seed Table 8), and all positive stimuli (left amygdala seed Table 9, right amygdala seed Table 10). Functional connectivity results located within the same region as the seed region due to auto-correlation effects have been included in the tables when they have been identified as a local maxima; however, these within-region correlations are most likely due to signal noise and smoothing during pre-processing and are not of interest when considering functional connectivity between regions. Additionally, local maxima have been reported in these tables; however, the difficulty in localizing significant activations or connectivity using cluster-extent based thresholding when clusters become large enough to span multiple brain regions must be taken into consideration when interpreting these

results. Cluster-extent based thresholding is limited by low spatial specificity which is especially problematic when large clusters spanning multiple regions are obtained. In this case, it is only possible to conclude that there is functional connectivity somewhere within the cluster and measures of statistical significance at specific points are unreliable (Woo et al., 2014).

Next, to determine whether emotional stimuli elicit enhanced functional connectivity between the amygdala and any other brain regions, functional connectivity for emotional stimuli was compared to functional connectivity for neutral stimuli. Contrary to expectations, no significant functional connectivity enhancement was observed for any of the conditions containing emotional stimuli compared to neutral stimuli (positive>neutral, negative>neutral, positive and negative>neutral, neutral>positive, neutral>negative, neutral>positive and negative, negative>positive, positive>negative).

Finally, to determine whether functional connectivity is enhanced between the amygdala and any other brain region as a function of both emotion and memory, functional connectivity was first assessed for the differences in memory conditions (positiveDM, negativeDM, neutralDM, emotionDM) and then neutral differences in memory were subtracted from emotional differences in memory (positiveDM>neutralDM, negativeDM>neutralDM, emotionDM>neutralDM, negativeDM>positiveDM, positiveDM>negativeDM). Contrary to expectations, no significant functional connectivity enhancement was found between either the left or right amygdala seed regions and medial temporal lobe regions, visual processing regions, the prefrontal cortex, or any other regions, for any of the successful emotional memory difference conditions compared to the neutral memory difference condition.

Taken together, these results suggest that viewing complex visual stimuli elicited widespread functional connectivity between both the left and right amygdala and numerous

regions throughout the brain. However, these patterns of functional connectivity were not enhanced for the emotional compared to the neutral conditions. Furthermore, functional connectivity between the amygdala and all other brain regions was not enhanced as a function of valence and memory.

Small volume correction.

To more fully understand the relationship between regional activations and functional connectivity for emotional processing and the emotional memory enhancement effect, SVC analyses were performed using *a priori* ROIs (bilateral amygdala and bilateral hippocampus) implementing specific *a priori* hypotheses. SVC analyses that looked at differences in valence, and differences in subsequent memory as a function of valence, were performed on the regional activation results. SVC analyses that looked at differences in subsequent memory as a function of valence were also performed on the functional connectivity correlation maps. The SVC functional connectivity analyses reported here supersede the previous whole brain functional connectivity analyses.

To investigate whether the amygdala exhibited enhanced emotional processing for emotional stimuli compared to neutral stimuli, a SVC analysis was performed using a bilateral amygdala mask on three regional activation contrasts of interest (positive and negative>neutral [Figure 5], negative>neutral [Figure 6], and positive>neutral [Figure 7]). As expected, all three emotional contrasts of interest found significant activations in both the left and right amygdala (Table 11).

To investigate the hypothesis that both the amygdala and hippocampus support memory enhancement for emotional information (McGaugh, 2004; Phelps, 2004), SVC analyses were performed using bilateral amygdala and bilateral hippocampus masks on the subsequent memory

contrasts of interest in which regional activations are greater for recalled stimuli than for not recalled stimuli which is known as the difference in memory effect (DM effect). These were considered first by memory (recalled – not recalled), then by valence, and finally emotional differences in memory were compared to neutral differences in memory to assess the emotional enhancement of memory (DM, negativeDM, positiveDM, emotionDM, neutralDM, negativeDM>neutralDM, positiveDM>neutralDM, emotionDM>neutralDM). The bilateral amygdala and bilateral hippocampal masks were applied separately to assess regional activations in these areas.

When a bilateral amygdala mask was applied to examine regional activation differences in memory as a function of valence, contrary to expectations, no suprathreshold clusters of activation were found in either the left or right amygdala for any of the emotional subsequent memory contrasts of interest. However, when a bilateral hippocampal mask was applied to examine differences in memory as a function of valence, significant activation was found in the left but not right hippocampus for successfully recalled items compared to not recalled items collapsed across valence (DM condition [Figure 8]) and for positive recalled items compared to positive not recalled items (positiveDM condition [Figure 9]), but no significant activations were found for any of the remaining contrasts of interest (Table 11). As expected, greater hippocampal activation was found for items that were recalled compared to not recalled; however, this effect seemed to be driven primarily by the positive DM condition as no significant hippocampal activation was observed for the negative DM or neutral DM conditions.

Finally, to test the amygdala modulation hypothesis that the amygdala modulates activity in the hippocampus to enhance memory for emotional information (McGaugh, 2004; Phelps, 2004), a SVC analysis was performed on amygdala seed region functional connectivity results as a

function of valence and memory with a bilateral hippocampal mask. Contrary to expectations, this direct test of functional connectivity between the amygdala and hippocampus found no voxels in either the left or right hippocampus that were significantly functionally connected with either the left or right amygdala for any of the subsequent memory by valence contrasts of interest.

Discussion

The current study used a beta series functional connectivity approach to examine differences in functional connectivity between the amygdala and the whole brain for general emotion processing and for the emotional enhancement of memory. Functional connectivity between left and right anatomical seed regions were compared to all other voxels in the brain during encoding of positive, negative, and neutral stimuli that were either later remembered or forgotten. To further elucidate the effects of valence and subsequent memory on regional activations and functional connectivity for the amygdala and hippocampus SVC analyses that focused on these regions were also performed.

Functional Connectivity

Because this study sought to distinguish valence effects on amygdala functional connectivity for emotional processing from subsequent memory, functional connectivity was investigated during presentation of positive, negative, and neutral stimuli without respect to subsequent memory. Widespread functional connectivity was observed between the amygdala and the rest of the brain for positive, negative, and neutral stimuli both combined and separately; however, no differences in functional connectivity were found between stimulus types. This finding contrasts with previous findings of increased connectivity between the amygdala and orbitofrontal cortex, dorsolateral prefrontal cortex, precuneus, cuneus, inferior temporal gyrus,

caudate, anterior cingulate cortex, insula, and hippocampus for positive stimuli compared to neutral stimuli and increased functional connectivity between the amygdala and striate and extrastriate visual cortices, temporal lobe (superior/middle/inferior temporal gyrus), parietal cortices, thalamus, hippocampus, parahippocampal gyrus, insula, anterior cingulate cortex, motor cortices, and somatosensory cortices for negative stimuli compared to neutral stimuli (Kang, Liu, Miskovic, Keil, & Ding, 2016). However, it should be noted that the current study had 36 trials for each emotion condition while the study by Kang et al. repeated the presentation of each picture five times resulting in 100 trials for each condition; thus, the low number of trials in the current study contributed to a decreased ability to detect differences in amygdala functional connectivity for emotional processing.

When functional connectivity was examined as a function of valence and subsequent memory, no significant differences in functional connectivity were found. Importantly, no differences for subsequently remembered emotional stimuli compared to subsequently remembered neutral stimuli were found regardless of valence. Further, no differences in functional connectivity were found for stimuli that were remembered compared to not remembered for any stimuli type. These findings are in contrast with previous findings of increased functional connectivity during successful encoding of emotional information compared to neutral information between the amygdala and multiple brain regions (Ritchey et al., 2011; Dolcos et al., 2004b; St. Jacques et al., 2009; Ritchey et al., 2008, Mickley Steinmetz et al., 2010). This finding is also contrary to expectations based on previous findings of differences in regional co-activations for subsequently remembered emotional stimuli compared to neutral stimuli (Hamann et al., 1999; Canli et al., 1999; Ritchey et al., 2011; Kensinger & Schacter, 2006; Dolcos et al., 2004; Murty et al., 2010).

Small Volume Correction

To investigate the critical role of the amygdala in emotion processing, SVC analyses were also performed on the regional activations observed during the presentation of positive, negative, and neutral pictures. Increased amygdala activity was observed for emotional stimuli compared to neutral stimuli when positive and negative stimuli were considered both separately and together. This finding is consistent with a metanalysis of 385 neuroimaging studies which reliably found increased amygdala activity in response to both positive and negative face, visual, auditory, olfactory, and gustatory stimuli compared to neutral stimuli (Costafreda, Brammer, David, & Fu, 2008). These findings are also consistent with previous findings of enhanced amygdala activation in response to emotional stimuli compared to neutral stimuli (Hamann et al., 1999; Canli et al., 1999; Kensinger & Schacter, 2006, Murty et al., 2010).

When a subsequent memory analysis was conducted for regional activations of the hippocampus, greater activity was observed in the left but not right hippocampus for positive items that were successfully recalled compared to not recalled. Increased activity in the left hippocampus was also seen for all remembered items, collapsed across valence, compared to all not remembered items. However, greater hippocampal activation was not observed for differences in memory for negative or neutral stimuli.

When regional activations of the amygdala were examined for subsequent memory; increased amygdala activity was not observed for subsequently remembered positive or negative items compared to neutral items. This held true when positive and negative stimuli were combined. Failure to find increased amygdala activity in response to subsequently remembered emotional stimuli contrasts with previous research which has consistently shown greater amygdala activity for positive, negative, and emotional items collapsed across valence that were

remembered compared to neutral items that were remembered (Hamann et al., 1999; Canli et al., 1999; Kensinger & Schacter, 2006; Murty et al., 2003). This may be a result of low statistical power due to a limited number of trials for each condition.

To examine the interactions between the amygdala and the hippocampus, SVC analyses were performed on the functional connectivity results. No differences in functional connectivity between either the left or right amygdala and bilateral hippocampus were observed for any of the emotional remembered stimuli compared to neutral stimuli regardless of valence. Further, no differences in functional connectivity were found for any of the successfully recalled items compared to not recalled items regardless of valence. This finding was contrary to expectations based on previous findings of regional co-activations (Murty et al., 2010) and the amygdala modulation hypothesis (McGaugh, 2004; Phelps, 2004). In the absence of findings of enhanced functional connectivity between the amygdala and the hippocampus, or any other brain region, for subsequently remembered emotional stimuli compared to neutral stimuli it must be considered that this study may have had insufficient power to observe potential differences in functional connectivity between conditions.

Limitations

The design of the current study may have resulted in low statistical power limiting our ability to find differences in functional connectivity. This study utilized an existing data set consisting of a single run with a limited number of trials per condition. As a result, several participants had to be excluded because they did not have a minimum of 8 trials of each type for the subsequent memory conditions. Furthermore, the limited number of trials per condition may have resulted in insufficient statistical power to find a true effect. Beta series analyses calculate a correlation coefficient for each trial, because the variance of the correlation coefficients is proportional to

the number of trials few trials results in high variance. Low statistical power may have also contributed to finding no greater amygdala activation for any of the emotional memory compared to neutral memory contrasts. Another limitation of this study may have been the use of a large anatomical amygdala seed region. The amygdala's role in enhancing processing and memory for emotional stimuli may be restricted to only a small region of amygdala such as the basolateral amygdala (Cahill & McGaugh, 1998; McGaugh & Roozendaal, 2002). Therefore, averaging signal across the entire amygdala may have led to partial volume effects reducing the ability of this study to observe significant activations and functional connectivity.

Future Directions

Because a network of regions is thought to facilitate the emotional enhancement of memory, additional seed regions such as the hippocampus and regions within the prefrontal cortex, such as the VLPFC and MPFC, may also help inform a greater understanding of how brain regions interact to facilitate the emotional enhancement of memory; however, this would require multiple comparison corrections for more regions which controls false positives but leads to the potential for more false negatives.

Differences in regional activations have been observed between men and women for emotional processing (Stevens & Hamann, 2012) as well as the emotional enhancement of memory (Cahill, Uncapher, Kilpatrick, Alkire, & Turner, 2004; Canli, Desmond, Zhao, & Gabrieli, 2002). Women have been shown to have greater activation than men in the left amygdala, left thalamus, hypothalamus, mammillary bodies, left caudate, and medial prefrontal cortex for negative stimuli; however, men had greater activation than women in the left amygdala, bilateral inferior frontal gyrus, and fusiform gyrus for positive stimuli (Stevens & Hamann, 2012). For subsequent memory, women but not men exhibited activity in the insula for

highly arousing negative pictures while men, but not women, had activations in the caudate, putamen, prefrontal cortex, and medial temporal lobe (Canli et al., 2002). A hemispheric laterality difference of amygdala activation for subsequently remembered negative such that women had increased activity in the left amygdala while men had increased activity in the right amygdala (Cahill et al., 2004). Thus, another interesting question for future research is whether there are sex-related differences in functional connectivity emotional processing and memory.

Older adults have shown a positivity effect such that positive stimuli are better remembered than negative stimuli (Mather, & Carstensen, 2005). However, the only known study to examine functional connectivity for subsequent emotional memory looked at the effects of negative stimuli (St. Jacques, Dolcos, & Cabeza, 2009). Therefore, future studies should expand on this line of research to investigate the effects of and valence on functional connectivity for subsequent memory in older adults.

Conclusion

In summary, this study sought to determine how the factors of positive and negative emotional valence may alter regional activations as well as functional connectivity between the amygdala and the hippocampus, and the amygdala and the whole brain, during emotional processing and emotional memory enhancement. This study is the first study, to our knowledge, to examine functional connectivity between the amygdala and the whole brain for the emotional memory enhancement effect as a function of valence. Widespread functional connectivity was observed for positive, negative, and neutral pictures; however, no differences in connectivity were observed between stimuli types. No differences in functional connectivity between the amygdala and either the hippocampus or the amygdala and the whole brain were observed for any subsequently remembered stimuli comparisons regardless of valence. Regional activations

were observed in bilateral amygdala for positive and negative stimuli compared to neutral stimuli both separately and combined; whereas, regional activations in the left but not right hippocampus were observed only for positive recalled stimuli compared to neutral stimuli and all recalled stimuli compared to all not recalled stimuli. Limitations which may have influenced this study's ability to make conclusions regarding functional connectivity included low statistical power due to a limited number of trials for each condition resulting in exclusion of participants and partial volume effects. Further research investigating emotional enhancement of memory is needed to elucidate how functional connectivity may differ as a function of valence.

References

Abivardi, A., & Bach, D. R. (2017). Deconstructing white matter connectivity of human amygdala nuclei with thalamus and cortex subdivisions in vivo. *Human brain mapping*, *38*(8), 3927-3940.

Adolphs, R., Cahill, L., Schul, R., & Babinsky, R. (1997). Impaired declarative memory for emotional material following bilateral amygdala damage in humans. *Learning & Memory*, *4*(3), 291-300.

Adolphs, R., Tranel, D., & Buchanan, T. W. (2005). Amygdala damage impairs emotional memory for gist but not details of complex stimuli. *Nature neuroscience*, *8*(4), 512.

Aggleton, J. P. (1986). A description of the amygdalo-hippocampal interconnections in the macaque monkey. *Experimental brain research*, *64*(3), 515-526.

Aggleton, J. P., Wright, N. F., Rosene, D. L., & Saunders, R. C. (2015). Complementary patterns of direct amygdala and hippocampal projections to the macaque prefrontal cortex. *Cerebral Cortex*, *25*(11), 4351-4373.

Alais, D., Newell, F. N., & Mamassian, P. (2010). Multisensory processing in review: from physiology to behaviour. *Seeing and perceiving*, *23*(1), 3-38.

Alemán-Gómez, Y., Melie-García, L., Valdés-Hernandez, P. (2006). IBASPM: toolbox for automatic parcellation of brain structures. *Presented at the 12th Annual Meeting of the Organization for Human Brain Mapping, June 11-15, 2006, Florence, Italy*. Available on CD-Rom in NeuroImage, Vol. 27, No.1.

Amaral, D. G., Behniea, H., & Kelly, J. L. (2003). Topographic organization of projections from the amygdala to the visual cortex in the macaque monkey. *Neuroscience*, *118*(4), 1099-1120.

Anderson, A. K., & Phelps, E. A. (2001). Lesions of the human amygdala impair enhanced perception of emotionally salient events. *Nature*, *411*(6835), 305.

Backs, R. W., da Silva, S. P., & Han, K. (2005). A comparison of younger and older adults' self-assessment manikin ratings of affective pictures. *Experimental aging research*, *31*(4), 421-440.

Balleine, B. W., Delgado, M. R., & Hikosaka, O. (2007). The role of the dorsal striatum in reward and decision-making. *Journal of Neuroscience*, *27*(31), 8161-8165.

Bechara, A., Damasio, H., Damasio, A. R., & Lee, G. P. (1999). Different contributions of the human amygdala and ventromedial prefrontal cortex to decision-making. *Journal of Neuroscience*, *19*(13), 5473-5481.

Berns, G. S., Bell, E., Capra, C. M., Prietula, M. J., Moore, S., Anderson, B., ... & Atran, S. (2012). The price of your soul: neural evidence for the non-utilitarian representation of sacred values. *Phil. Trans. R. Soc. B*, *367*(1589), 754-762.

Brett, M., Anton, J. L., Valabregue, R., & Poline, J. B. (2002). Region of interest analysis using the MarsBar toolbox for SPM 99. *Neuroimage*, *16*(2), S497.

Brierley, B., Medford, N., Shaw, P., & David, A. S. (2004). Emotional memory and perception in temporal lobectomy patients with amygdala damage. *Journal of Neurology, Neurosurgery & Psychiatry*, *75*(4), 593-599.

Bush, G., Vogt, B. A., Holmes, J., Dale, A. M., Greve, D., Jenike, M. A., & Rosen, B. R. (2002). Dorsal anterior cingulate cortex: a role in reward-based decision making. *Proceedings of the National Academy of Sciences*, *99*(1), 523-528.

Cahill, L. (1997). The neurobiology of emotionally influenced memory implications for understanding traumatic memory. *Annals of the New York Academy of Sciences*, *821*(1), 238-246.

Cahill, L., Babinsky, R., Markowitsch, H. J., & McGaugh, J. L. (1995). The amygdala and emotional memory. *Nature*.

Cahill, L., & McGaugh, J. L. (1998). Mechanisms of emotional arousal and lasting declarative memory. *Trends in neurosciences*, *21*(7), 294-299.

Cahill, L., Uncapher, M., Kilpatrick, L., Alkire, M. T., & Turner, J. (2004). Sex-related hemispheric lateralization of amygdala function in emotionally influenced memory: an FMRI investigation. *Learning & memory*, *11*(3), 261-266.

Canli, T., Desmond, J. E., Zhao, Z., & Gabrieli, J. D. (2002). Sex differences in the neural basis of emotional memories. *Proceedings of the National Academy of Sciences*, *99*(16), 10789-10794.

Canli, T., Zhao, Z. U. O., Desmond, J. E., Glover, G., & Gabrieli, J. D. (1999). fMRI identifies a network of structures correlated with retention of positive and negative emotional memory. *Psychobiology*, *27*(4), 441-452.

Cavanna, A. E., & Trimble, M. R. (2006). The precuneus: a review of its functional anatomy and behavioural correlates. *Brain*, *129*(3), 564-583.

Cohen, J., MacWhinney, B., Flatt, M., & Provost, J. (1993). PsyScope: An interactive graphic system for designing and controlling experiments in the psychology laboratory using Macintosh computers. *Behavior Research Methods, Instruments, & Computers*, *25*(2), 257-271.

Costafreda, S. G., Brammer, M. J., David, A. S., & Fu, C. H. (2008). Predictors of amygdala activation during the processing of emotional stimuli: a meta-analysis of 385 PET and fMRI studies. *Brain research reviews*, *58*(1), 57-70.

Davis, M., & Whalen, P. J. (2001). The amygdala: vigilance and emotion. *Molecular psychiatry*, *6*(1), 13.

Dolcos, F., Denkova, E., & Dolcos, S. (2012). Neural correlates of emotional memories: a review of evidence from brain imaging studies. *Psychologia*, *55*(2), 80-111.

Dolcos, F., LaBar, K. S., & Cabeza, R. (2004a). Dissociable effects of arousal and valence on prefrontal activity indexing emotional evaluation and subsequent memory: an event-related fMRI study. *Neuroimage*, *23*(1), 64-74.

Dolcos, F., LaBar, K. S., & Cabeza, R. (2004b). Interaction between the amygdala and the medial temporal lobe memory system predicts better memory for emotional events. *Neuron*, *42*(5), 855-863.

Edmiston, E. K., McHugo, M., Dukic, M. S., Smith, S. D., Abou-Khalil, B., Eggers, E., & Zald, D. H. (2013). Enhanced visual cortical activation for emotional stimuli is preserved in patients with unilateral amygdala resection. *Journal of Neuroscience*, *33*(27), 11023-11031.

Eickhoff, S. B., Stephan, K. E., Mohlberg, H., Grefkes, C., Fink, G. R., Amunts, K., & Zilles, K. (2005). A new SPM toolbox for combining probabilistic cytoarchitectonic maps and functional imaging data. *Neuroimage*, *25*(4), 1325-1335.

Epstein, R. A. (2008). Parahippocampal and retrosplenial contributions to human spatial navigation. *Trends in cognitive sciences*, *12*(10), 388-396.

Fellows, L. K., & Farah, M. J. (2007). The role of ventromedial prefrontal cortex in decision making: judgment under uncertainty or judgment per se?. *Cerebral Cortex*, *17*(11), 2669-2674.

Friedman, D. P., Murray, E. A., O'Neill, J. B., & Mishkin, M. (1986). Cortical connections of the somatosensory fields of the lateral sulcus of macaques: evidence for a corticolimbic pathway for touch. *Journal of Comparative Neurology*, *252*(3), 323-347.

Friston, K. J., Buechel, C., Fink, G. R., Morris, J., Rolls, E., & Dolan, R. J. (1997). Psychophysiological and modulatory interactions in neuroimaging. *Neuroimage*, *6*(3), 218-229.

Friston, K. J., Holmes, A. P., Worsley, K. J., Poline, J. P., Frith, C. D., & Frackowiak, R. S. (1994). Statistical parametric maps in functional imaging: a general linear approach. *Human brain mapping*, *2*(4), 189-210.

Gläscher, J., & Adolphs, R. (2003). Processing of the arousal of subliminal and supraliminal emotional stimuli by the human amygdala. *Journal of Neuroscience*, *23*(32), 10274-10282.

Göttlich, M., Beyer, F., & Krämer, U. (2015). BASCO: a toolbox for task-related functional connectivity. *Frontiers in systems neuroscience*, *9*, 126.

Haines, Duane E. (2012). *Neuroanatomy: An atlas of structures, sections, and systems*. (8th ed.). Lippincott Williams & Wilkins.

Hamani, C., Mayberg, H., Stone, S., Laxton, A., Haber, S., & Lozano, A. M. (2011). The subcallosal cingulate gyrus in the context of major depression. *Biological psychiatry*, *69*(4), 301-308.

Hamann, S. (2001). Cognitive and neural mechanisms of emotional memory. *Trends in cognitive sciences*, *5*(9), 394-400.

Hamann, S. B., Ely, T. D., Grafton, S. T., & Kilts, C. D. (1999). Amygdala activity related to enhanced memory for pleasant and aversive stimuli. *Nature neuroscience*, *2*(3), 289.

Hamann, S., Stevens, J., Vick, J. H., Bryk, K., Quigley, C. A., Berenbaum, S. A., & Wallen, K. (2014). Brain responses to sexual images in 46, XY women with complete androgen insensitivity syndrome are female-typical. *Hormones and behavior*, *66*(5), 724-730.

Hermundstad, A. M., Bassett, D. S., Brown, K. S., Aminoff, E. M., Clewett, D., Freeman, S., Frithsen, A., Johnson, A., Tipper, C. M., Miller, M. B., Grafton, S. T., & Carlson, J.M. (2013). Structural foundations of resting-state and task-based functional connectivity in the human brain. *Proceedings of the National Academy of Sciences*, *110*(15), 6169-6174.

Hurlburt, R. T., Alderson-Day, B., Fernyhough, C., & Kühn, S. (2015). What goes on in the resting-state? A qualitative glimpse into resting-state experience in the scanner. *Frontiers in psychology*, *6*, 1535.

Josephs, O., Turner, R., & Friston, K. (1997). Event-related fMRI. *Human brain mapping*, *5*(4), 243-248.

Kane, M. J., & Engle, R. W. (2002). The role of prefrontal cortex in working-memory capacity, executive attention, and general fluid intelligence: An individual-differences perspective. *Psychonomic bulletin & review*, *9*(4), 637-671.

Kang, D., Liu, Y., Miskovic, V., Keil, A., & Ding, M. (2016). Large- scale functional brain connectivity during emotional engagement as revealed by beta- series correlation analysis. *Psychophysiology*, *53*(11), 1627-1638.

Kensinger, E. A., & Corkin, S. (2004). Two routes to emotional memory: Distinct neural processes for valence and arousal. *Proceedings of the National Academy of Sciences of the United States of America*, *101*(9), 3310-3315.

Kensinger, E. A., & Schacter, D. L. (2006). Processing emotional pictures and words: effects of valence and arousal. *Cognitive, Affective, & Behavioral Neuroscience*, *6*(2), 110-126.

Kensinger, E. A., & Schacter, D. L. (2008). Neural processes supporting young and older adults' emotional memories. *Journal of cognitive neuroscience*, *20*(7), 1161-1173.

Knutson, B., Adams, C. M., Fong, G. W., & Hommer, D. (2001). Anticipation of increasing monetary reward selectively recruits nucleus accumbens. *Journal of Neuroscience*, *21*(16), RC159-RC159.

Krauzlis, R. J., Liston, D., & Carello, C. D. (2004). Target selection and the superior colliculus: goals, choices and hypotheses. *Vision research*, *44*(12), 1445-1451.

Krauzlis, R. J., Lovejoy, L. P., & Zénon, A. (2013). Superior colliculus and visual spatial attention. *Annual review of neuroscience*, *36*, 165-182.

Lancaster, J. L. (1997). The Talairach Daemon, a database server for Talairach atlas labels. *Neuroimage*, *5*, S633.

Lancaster, J. L., Rainey, L. H., Summerlin, J L, Freitas, C S, Fox, P T, Evans, A. C., … Mazziotta, J. C. M. (1997). Automated Labeling of the Human Brain: A Preliminary Report on the Development and Evaluation of a Forward-Transform Method, 5.

Lancaster, J. L., Woldorff, M. G., Parsons, L. M., Liotti, M., Freitas, C. S., Rainey, L., Kochunov, P.V., Nickerson, D., Mikiten, S.A., & Fox, P. T. (2000). Automated Talairach atlas labels for functional brain mapping. *Human brain mapping*, *10*(3), 120-131.

Lang, P. J., Bradley, M. M., & Cuthbert, B. N. (1997). International affective picture system (IAPS): Technical manual and affective ratings. *NIMH Center for the Study of Emotion and Attention*, 39-58.

Maguire, E. (2001). The retrosplenial contribution to human navigation: a review of lesion and neuroimaging findings. *Scandinavian journal of psychology*, *42*(3), 225-238.

Maldjian, J. A., Laurienti, P. J., Kraft, R. A., & Burdette, J. H. (2003). An automated method for neuroanatomic and cytoarchitectonic atlas-based interrogation of fMRI data sets. *Neuroimage*, *19*(3), 1233-1239.

Maldjian JA, Laurienti PJ, Burdette JH. (2004). Precentral Gyrus Discrepancy in Electronic Versions of the Talairach Atlas. *Neuroimage, 21*(1), 450-455.

Mather, M., & Carstensen, L. L. (2005). Aging and motivated cognition: The positivity effect in attention and memory. *Trends in cognitive sciences*, *9*(10), 496-502.

McGaugh, J. L. (2000). Memory--a century of consolidation. *Science*, *287*(5451), 248-251.

McGaugh, J. L. (2004). The amygdala modulates the consolidation of memories of emotionally arousing experiences. *Annu. Rev. Neurosci.*, *27*, 1-28.

McGaugh, J. L., & Roozendaal, B. (2002). Role of adrenal stress hormones in forming lasting memories in the brain. *Current opinion in neurobiology*, *12*(2), 205-210.

Mickley, K. R., & Kensinger, E. A. (2008). Emotional valence influences the neural correlates associated with remembering and knowing. *Cognitive, Affective, & Behavioral Neuroscience*, *8*(2), 143-152.

Mickley Steinmetz, K. R., Addis, D. R., & Kensinger, E. A. (2010). The effect of arousal on the emotional memory network depends on valence. *Neuroimage*, *53*(1), 318-324.

Murty, V. P., Ritchey, M., Adcock, R. A., & LaBar, K. S. (2010). fMRI studies of successful emotional memory encoding: A quantitative meta-analysis. *Neuropsychologia*, *48*(12), 3459-3469.

Nichols, T. E., & Holmes, A. P. (2002). Nonparametric permutation tests for functional neuroimaging: a primer with examples. *Human brain mapping*, *15*(1), 1-25.

Paller, K. A., & Wagner, A. D. (2002). Observing the transformation of experience into memory. *Trends in cognitive sciences*, *6*(2), 93-102.

Phelps, E. A. (2004). Human emotion and memory: interactions of the amygdala and hippocampal complex. *Current opinion in neurobiology*, *14*(2), 198-202.

Phelps, E. A., LaBar, K. S., Anderson, A. K., O'connor, K. J., Fulbright, R. K., & Spencer, D. D. (1998). Specifying the contributions of the human amygdala to emotional memory: A case study. *Neurocase*, *4*(6), 527-540.

Phelps, E. A., & LeDoux, J. E. (2005). Contributions of the amygdala to emotion processing: from animal models to human behavior. *Neuron*, *48*(2), 175-187.

Piech, R. M., McHugo, M., Smith, S. D., Dukic, M. S., Van Der Meer, J., Abou-Khalil, B., Most, S. B., & Zald, D. H. (2011). Attentional capture by emotional stimuli is preserved in patients with amygdala lesions. *Neuropsychologia*, *49*(12), 3314-3319.

Poldrack, R. A. (2007). Region of interest analysis for fMRI. *Social cognitive and affective neuroscience*, *2*(1), 67-70.

Pruim, R. H., Mennes, M., Buitelaar, J. K., & Beckmann, C. F. (2015). Evaluation of ICA-AROMA and alternative strategies for motion artifact removal in resting state fMRI. *Neuroimage*, *112*, 278-287.

Pruim, R. H., Mennes, M., van Rooij, D., Llera, A., Buitelaar, J. K., & Beckmann, C. F. (2015). ICA-AROMA: A robust ICA-based strategy for removing motion artifacts from fMRI data. *Neuroimage*, *112*, 267-277.

Reisberg, D., & Heuer, F. (2004). Remembering emotional events. In D. Reisberg & P. Hertel (Eds.), Series in affective science. Memory and emotion (pp. 3–41). New York: Oxford University Press.

Rissman, J., Gazzaley, A., & D'esposito, M. (2004). Measuring functional connectivity during distinct stages of a cognitive task. *Neuroimage*, *23*(2), 752-763.

Ritchey, M., Dolcos, F., & Cabeza, R. (2008). Role of amygdala connectivity in the persistence of emotional memories over time: An event-related fMRI investigation. *Cerebral Cortex*, *18*(11), 2494-2504.

Ritchey, M., LaBar, K. S., & Cabeza, R. (2011). Level of processing modulates the neural correlates of emotional memory formation. *Journal of Cognitive Neuroscience*, *23*(4), 757-771.

Rolls, E. T., Joliot, M., & Tzourio-Mazoyer, N. (2015). Implementation of a new parcellation of the orbitofrontal cortex in the automated anatomical labeling atlas. *Neuroimage*, *122*, 1-5.

Sporns, O. (2013). Structure and function of complex brain networks. *Dialogues in clinical neuroscience*, *15*(3), 247.

Sporns, O., Chialvo, D. R., Kaiser, M., & Hilgetag, C. C. (2004). Organization, development and function of complex brain networks. *Trends in cognitive sciences*, *8*(9), 418-425.

Squire, L. R., & Zola-Morgan, S. (1991). The medial temporal lobe memory system. *Science*, *253*(5026), 1380-1386.

Stevens, J. S., & Hamann, S. (2012). Sex differences in brain activation to emotional stimuli: a meta-analysis of neuroimaging studies. *Neuropsychologia*, *50*(7), 1578-1593.

St. Jacques, P. L., Dolcos, F., & Cabeza, R. (2009). Effects of aging on functional connectivity of the amygdala for subsequent memory of negative pictures: a network analysis of functional magnetic resonance imaging data. *Psychological science*, *20*(1), 74-84.

Tzourio-Mazoyer N, Landeau B, Papathanassiou D, Crivello F, Etard O, Delcroix N, Mazoyer B, Joliot M. (2002). Automated anatomical labeling of activations in SPM using a macroscopic anatomical parcellation of the MNI MRI single-subject brain. *Neuroimage, 15*(1), 273-89.

Van Den Heuvel, M. P., & Pol, H. E. H. (2010). Exploring the brain network: a review on resting-state fMRI functional connectivity. European neuropsychopharmacology, 20(8), 519-534.

Vuilleumier, P. (2005). How brains beware: neural mechanisms of emotional attention. *Trends in cognitive sciences*, *9*(12), 585-594.

Wagner, A. D., Maril, A., Bjork, R. A., & Schacter, D. L. (2001). Prefrontal contributions to executive control: fMRI evidence for functional distinctions within lateral prefrontal cortex. *Neuroimage*, *14*(6), 1337-1347.

Woo, C. W., Krishnan, A., & Wager, T. D. (2014). Cluster-extent based thresholding in fMRI analyses: pitfalls and recommendations. *Neuroimage*, *91*, 412-419.

Yarkoni, T., Poldrack, R. A., Nichols, T. E., Van Essen, D. C., & Wager, T. D. (2011). Large-scale automated synthesis of human functional neuroimaging data. *Nature methods*, *8*(8), 665.

Yukie, M. (2002). Connections between the amygdala and auditory cortical areas in the macaque monkey. *Neuroscience research*, *42*(3), 219-229.

Zhuang, J., Peltier, S., He, S., LaConte, S., & Hu, X. (2008). Mapping the connectivity with structural equation modeling in an fMRI study of shape-from-motion task. *Neuroimage*, *42*(2), 799-806.

Figures

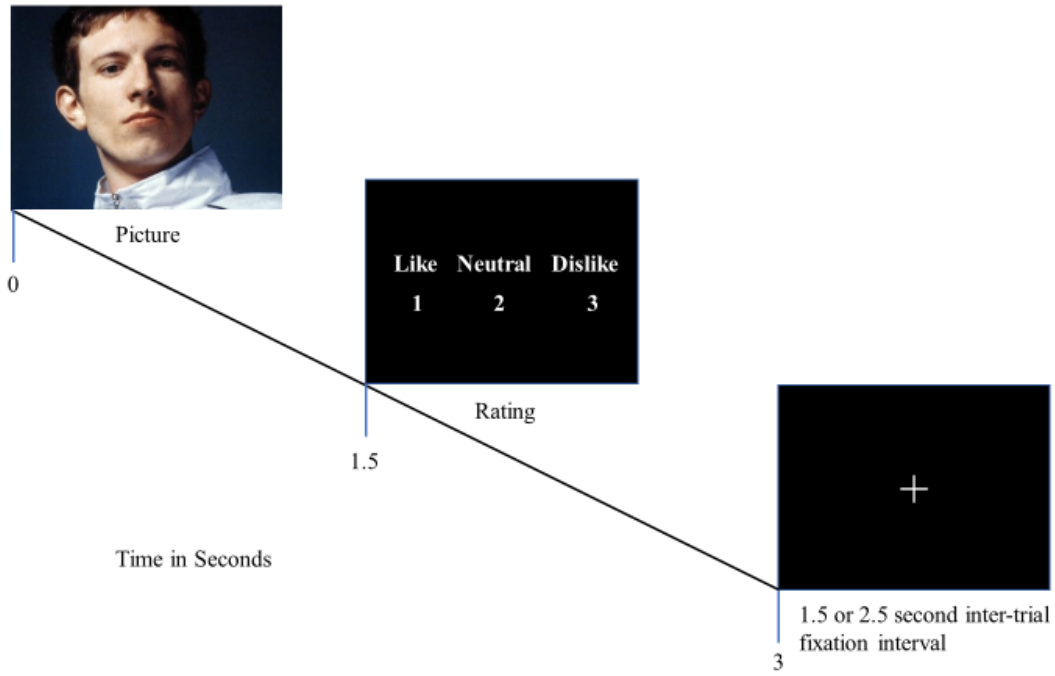

Figure 1. Design of experimental trials. Positive, negative, and neutral pictures were presented pseudo-randomly for 1.5 s each. Next, a ratings screen was presented for 1.5 seconds followed by an inter-trial fixation interval during which a white "+" on a black background was presented for either 1.5 or 2.5 seconds (pseudorandomly distributed across trials).

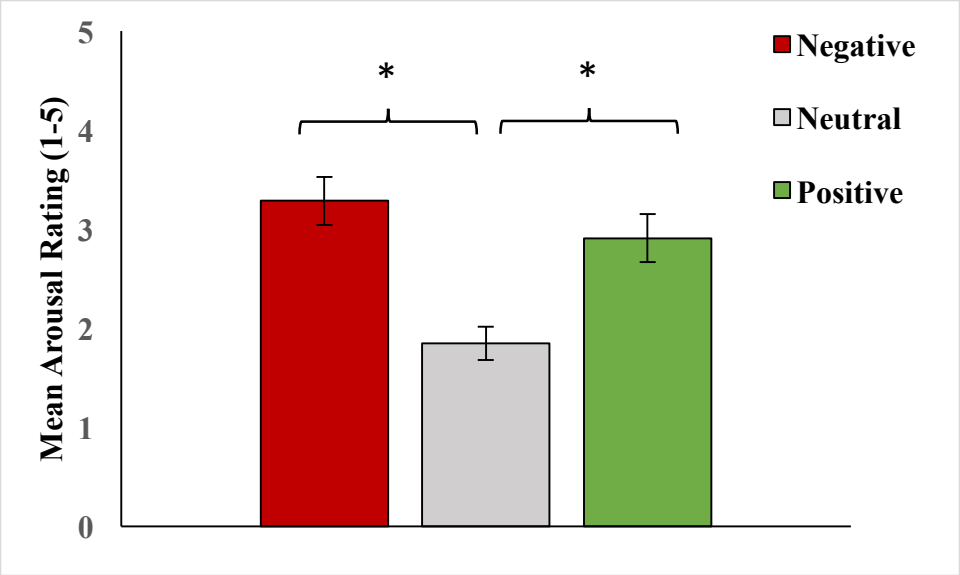

Figure 2. Mean arousal ratings of stimuli as a function of valence. Significant differences in subjects' mean arousal ratings were found between negative and neutral stimuli $p = .002$ and between positive and neutral stimuli $p < .001$. These significant findings are marked with an *.

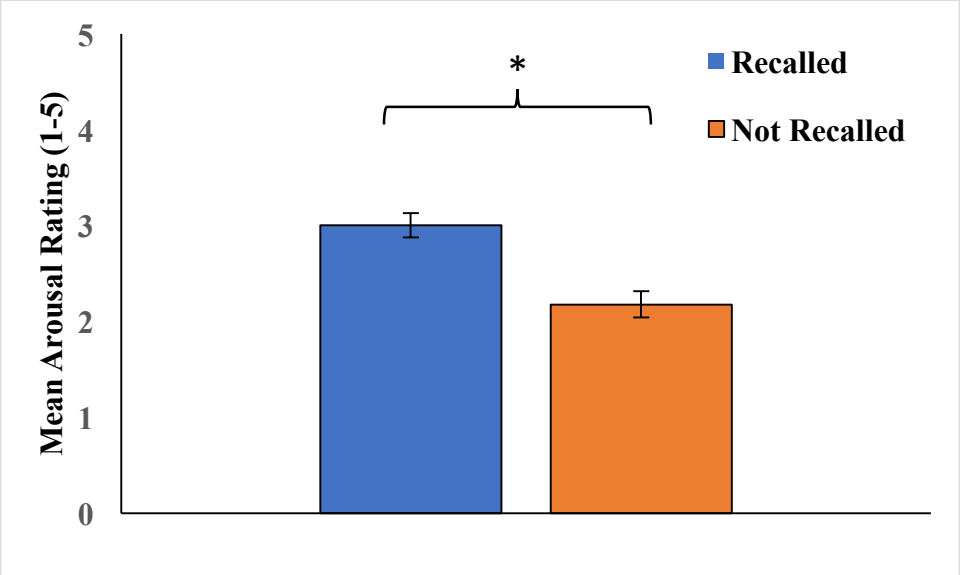

Figure 3. Mean arousal ratings of stimuli as a function of memory. Significant differences in subjects' mean arousal ratings were found between stimuli that were recalled and those that were not recalled $p = .001$. This significant finding is marked with an *.

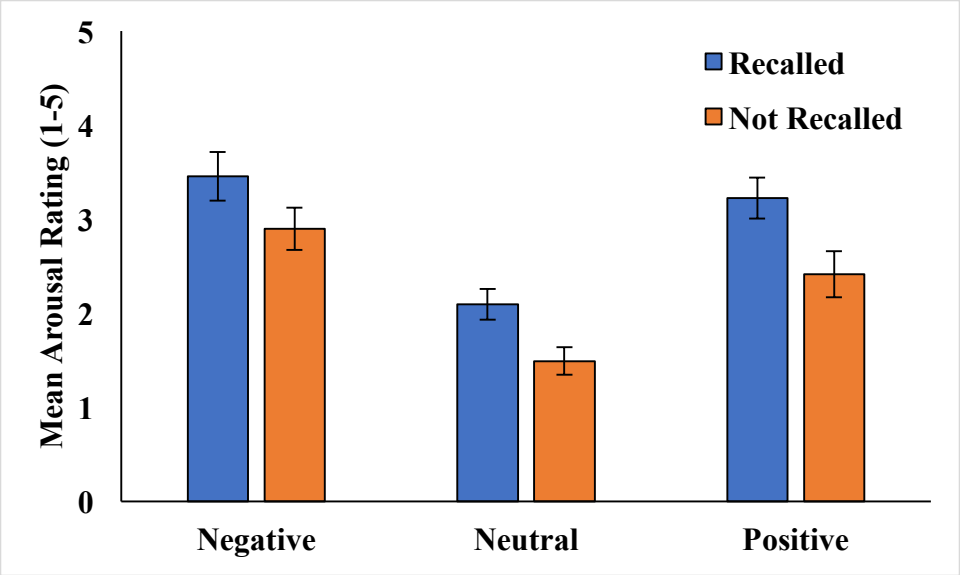

Figure 4. Mean arousal ratings of stimuli as a function of valence and memory. No significant differences were found in arousal ratings between negative recalled and negative not recalled stimuli, between neutral recalled stimuli and neutral not recalled stimuli, or between positive recalled stimuli and positive not recalled stimuli.

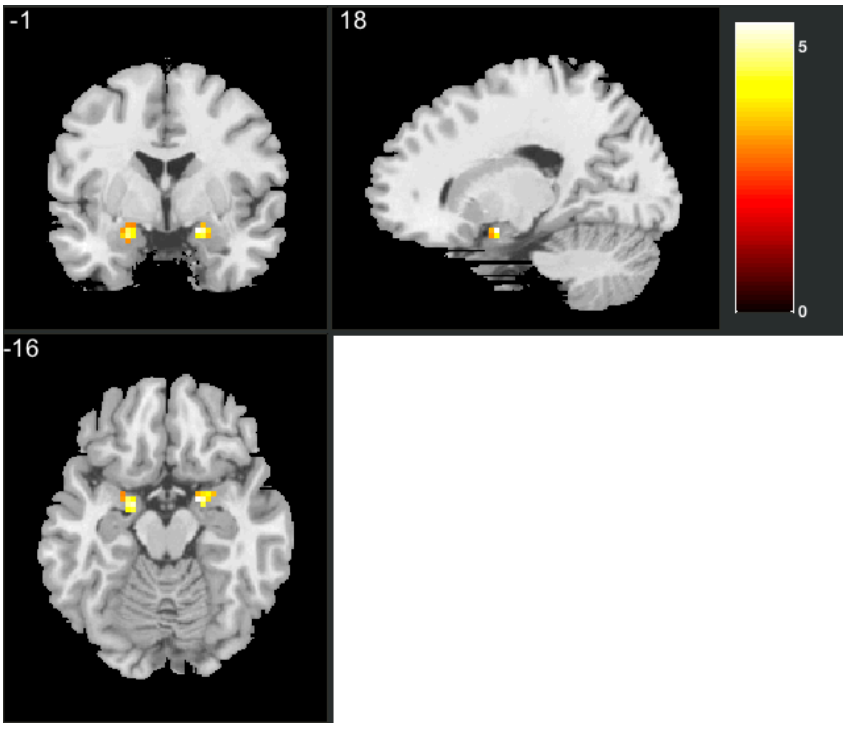

Figure 5. Small volume correction for the positive and negative > neutral contrast. Activation for the peak voxel in the right amygdala $t > 3.0100$; $p < 0.0500$; critical suprathreshold cluster size = 1.

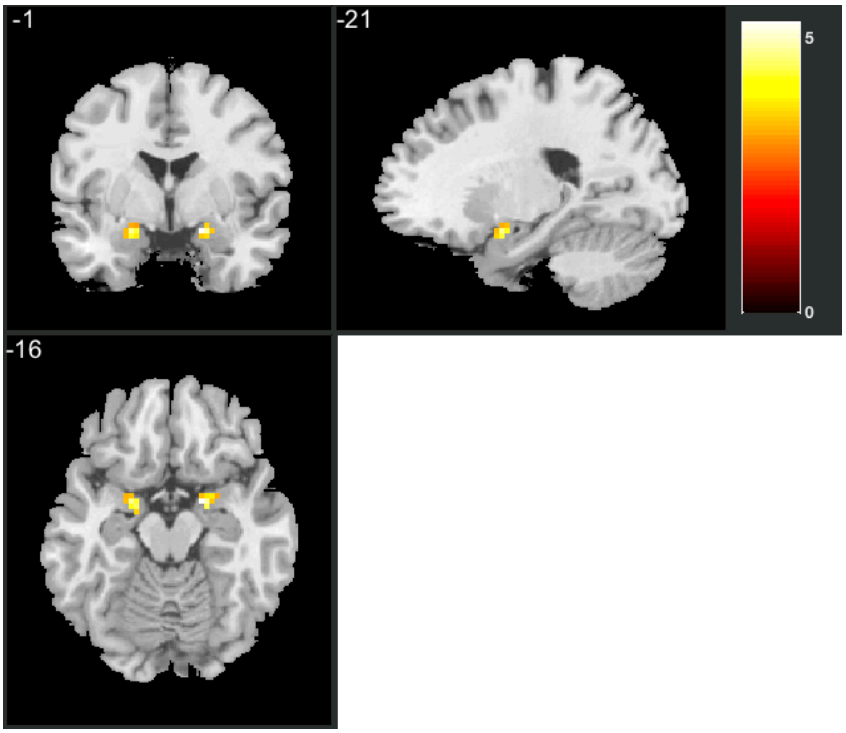

Figure 6. Small volume correction for the negative > neutral contrast. Activation for the peak voxel in the left amygdala t > 3.0100; p < 0.0500; critical suprathreshold cluster size = 1.

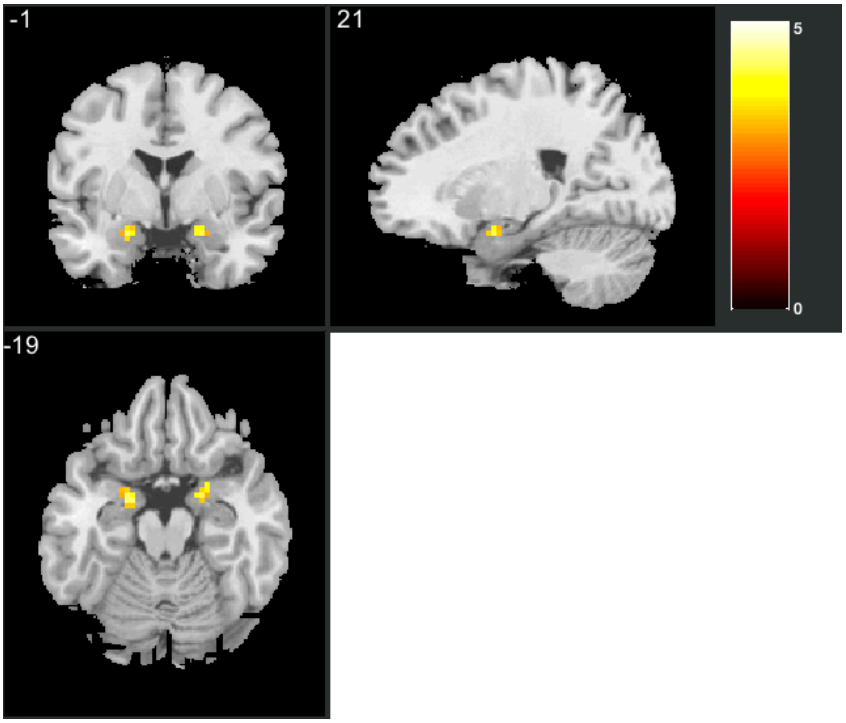

Figure 7. Small volume correction for the positive > neutral contrast. Activation for the peak voxel in the right amygdala t > 3.0100; p < 0.0500; critical suprathreshold cluster size = 1.

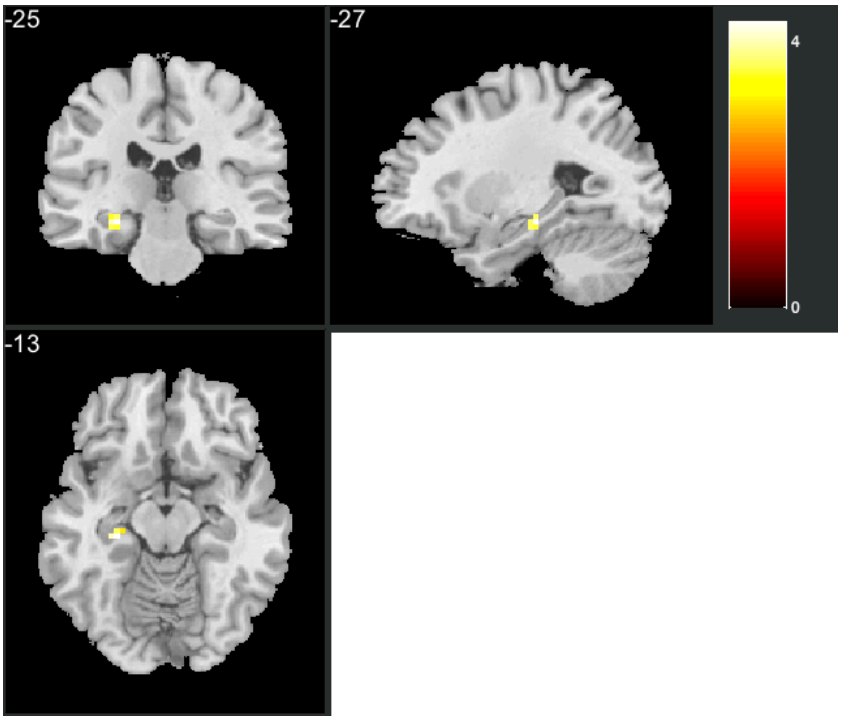

Figure 8. Small volume correction for the DM contrast. Activation for the peak voxel in the left hippocampus $t > 3.0100$; $p < 0.0500$; critical suprathreshold cluster size = 4.

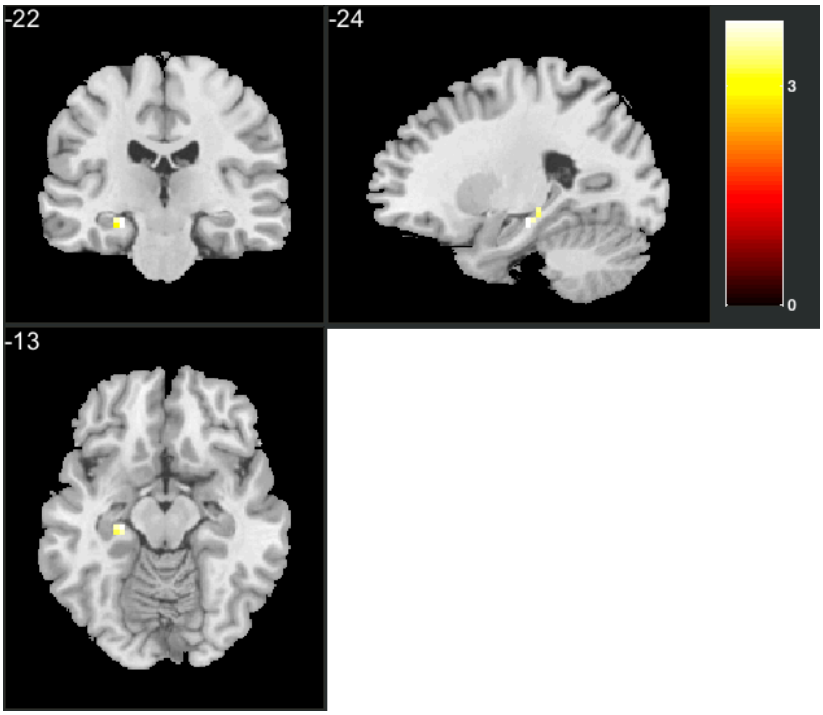

Figure 9. Small volume correction for the positive DM contrast. Activation for the peak voxel in the left hippocampus $t > 3.0100$; $p < 0.0500$; critical suprathreshold cluster size = 4.

Tables

Table 1

Functional Connectivity for All Stimuli with Left Amygdala Seed Region

		Pseudo	MNI Coordinates			
Region Label	L/R	t-value	x	y	z	Extent
Amygdala	L	8.368	-18	-4	-19	6966
Angular gyrus	L	5.469	-39	-61	23	
Calcarine fissure and surrounding cortex	L	4.706	3	-82	-4	
Caudate nucleus	L	4.356	-9	5	-1	
Cerebellum crus I	L	5.399	-42	-64	-25	
Cerebellum lobule IV, V	L	4.553	-12	-55	-16	
Cerebellum lobule VI	L	5.349	-9	-70	-19	
Cerebellum lobule VI	R	5.690	9	-79	-19	
Cuneus	L	4.878	-9	-88	32	
Cuneus	R	4.967	12	-91	20	
Fusiform gyrus	L	5.321	-36	-43	-25	
Fusiform gyrus	R	6.404	27	-70	-13	
Inferior occipital gyrus	R	4.468	42	-82	-13	
Inferior temporal gyrus	L	5.601	-48	-61	-13	
Inferior temporal gyrus	R	5.653	60	-61	-4	
Insula	L	5.469	-42	2	2	
Lingual gyrus	L	4.812	-9	-64	-7	
Lingual gyrus	R	5.514	27	-64	-4	
Middle cingulate & paracingulate gyri	L	4.813	0	-22	41	
Middle cingulate & paracingulate gyri	R	5.591	3	23	29	
Middle occipital gyrus	L	5.822	-42	-76	-1	
Middle temporal gyrus	L	6.129	-54	-55	14	
Middle temporal gyrus	R	6.204	51	-43	2	
Parahippocampal gyrus	L	5.113	-27	-28	-16	
Postcentral gyrus	R	4.849	15	-43	59	
Precentral gyrus	R	5.265	27	-22	53	
Precuneus	L	5.312	0	-55	14	
Precuneus	R	5.920	18	-64	44	
Rolandic operculum	R	4.535	48	-22	20	
Superior frontal gyrus, dorsolateral	L	4.274	-24	5	65	
Superior frontal gyrus, dorsolateral	R	5.287	39	-4	62	
Superior frontal gyrus, medial	R	4.836	6	20	44	
Superior parietal lobule	L	4.772	-24	-58	44	
Superior parietal lobule	R	4.915	27	-58	47	
Superior temporal gyrus	L	4.949	-60	-1	2	
Superior temporal gyrus	R	4.989	60	-25	14	
Supplementary motor area	L	5.853	-9	-13	50	
Supplementary motor area	R	5.482	3	5	56	
Temporal pole: superior temporal gyrus	L	4.938	-54	14	-10	
Vermis lobule VI	R	4.939	3	-64	-22	
Amygdala	R	5.423	33	-1	-13	398
Hippocampus	R	4.938	18	-4	-13	
Insula	R	4.774	39	5	-16	
Lenticular nucleus, Putamen	R	5.803	27	5	-13	
Midbrain	L	3.823	-3	-22	-16	
Middle temporal gyrus	R	3.954	54	-1	-19	
Olfactory cortex	R	4.227	18	8	-16	
Parahippocampal gyrus	R	4.509	24	-13	-28	

Temporal pole: middle temporal gyrus	R	3.393	57	8	-19	
Temporal pole: superior temporal gyrus	R	4.681	30	5	-22	
Inferior frontal gyrus, pars opercularis	R	3.469	45	8	23	224
Middle temporal gyrus	R	4.233	57	-22	-10	
Postcentral gyrus	R	4.579	63	-7	20	
Precentral gyrus	R	4.055	60	8	23	
Rolandic operculum	R	4.084	60	-4	11	
Superior temporal gyrus	R	4.466	57	-13	-10	
Temporal pole: superior temporal gyrus	R	4.024	63	8	-1	
Inferior parietal gyrus, excluding supramarginal and angular gyri	L	3.594	-33	-31	35	223
Lenticular nucleus, Putamen	L	3.680	-27	-16	11	
Middle temporal gyrus	L	3.946	-60	-34	2	
Postcentral gyrus	L	3.873	-66	-22	35	
Rolandic operculum	L	4.957	-39	-28	20	
Superior temporal gyrus	L	4.974	-63	-31	14	
Supramarginal gyrus	L	5.231	-60	-28	26	
Inferior parietal gyrus, excluding supramarginal and angular gyri	L	3.927	-51	-37	53	180
Insula	R	3.560	39	-13	-4	
Lenticular nucleus, Pallidum	R	4.015	15	-4	-1	
Lenticular nucleus, Putamen	R	4.333	30	-13	8	
Postcentral gyrus	L	4.472	-33	-40	65	
Precentral gyrus	L	4.903	-27	-19	68	
Thalamus	L	4.578	-3	-19	11	
Thalamus	R	4.377	12	-19	5	
Anterior cingulate gyrus	L	3.620	-6	38	5	171
Gyrus rectus	L	4.184	-6	44	-19	
Superior frontal gyrus, dorsolateral	L	4.532	-12	65	17	
Superior frontal gyrus, medial	L	5.394	0	65	20	
Superior frontal gyrus, medial	R	4.035	3	56	14	
Superior frontal gyrus, medial orbital	L	4.817	-6	44	-10	
Inferior frontal gyrus, pars triangularis	L	3.551	-48	32	23	112
Middle frontal gyrus	L	4.615	-45	41	23	
Superior frontal gyrus, dorsolateral	L	4.063	-27	44	38	
Postcentral gyrus	L	4.485	-51	-10	32	105
Superior frontal gyrus, dorsolateral	R	4.233	24	41	38	96
Superior frontal gyrus, medial	L	4.902	0	53	38	
Superior frontal gyrus, medial	R	4.482	12	50	47	
Inferior frontal gyrus, pars orbitalis	R	4.299	42	26	-13	86
Insula	R	3.423	39	17	-7	
Lateral orbital gyrus	R	3.731	48	35	-16	
Temporal pole: superior temporal gyrus	R	4.814	45	17	-22	
Inferior frontal gyrus, pars triangularis	R	4.293	51	35	17	82
Middle frontal gyrus	R	3.204	33	8	59	56
Superior frontal gyrus, dorsolateral	R	5.104	24	14	56	
Supplementary motor area	R	3.990	18	11	65	
Middle frontal gyrus	L	4.549	-45	50	11	52

Note. Table shows one local maxima for each region within each cluster that is separated by more than 8mm. Regions are reported separately for each hemisphere and up to 50 peaks are reported per cluster. Regions were automatically labeled using the BSPMview (http://www.bobspunt.com/bspmview/) implementation of the AAL2 brain parcellation (Rolls, Joliot, & Tzourio-Mazoyer, 2015). Regions not identified by BSPMview (DOI 10.5281/zenodo.168074) with AAL2 were identified based on neuroanatomical examination with the BSPMview implementation of AAL Toolbox (Eickhoff et al., 2005); WFU Pickatlas Individual brain atlases using AAL (Tzourio-Mazoyer et al., 2002), IBASPM71 (Alemán-Gómez, Melie-García, & Valdés-Hernandez, 2006), Talairach Daemon (TD Labels, TD lobes, TD Brodmann areas+) (Lancaster, 1997; Lancaster et al., 1997; Lancaster et al., 2000); Haines Neuroanatomy Atlas (Haines, 2012); and coordinate association in Neurosynth (http://www.neurosynth.org/) (Yarkoni, Poldrack, Nichols, Van Essen, & Wager, 2011). Local maxima are reported with

Montreal Neurological Institute (MNI) coordinates x, y, and z in the left-right, anterior-posterior, and inferior-superior dimensions, respectively. Maximal Pseudo-T statistics, and extent in voxels (k) are reported for all significant clusters (cluster defining threshold = 3.01, cluster threshold FWE-corrected $p<0.05$; critical suprathreshold cluster size =43).

Table 2

Functional Connectivity for All Stimuli with Right Amygdala Seed Region

		Psuedo t-	MNI Coordinates			
Region Label	L/R	value	x	y	z	Extent
Amygdala	R	9.36	24	2	-16	7310
Calcarine fissure and surrounding cortex	L	5.48	-21	-64	8	
Calcarine fissure and surrounding cortex	R	5.42	6	-82	-1	
Cerebellum lobule VI	R	5.46	33	-61	-22	
Cuneus	L	5.01	0	-79	20	
Cuneus	R	5.05	9	-64	20	
Fusiform gyrus	L	5.39	-30	-67	-19	
Fusiform gyrus	R	6.70	30	-73	-16	
Hippocampus	L	4.97	-24	-19	-19	
Hippocampus	R	5.75	21	-16	-16	
Insula	L	4.83	-42	-1	-1	
Lenticular nucleus, Putamen	L	5.49	-30	-13	2	
Lingual gyrus	L	5.05	-9	-61	-1	
Middle occipital gyrus	L	5.65	-33	-82	2	
Middle occipital gyrus	R	5.60	42	-73	2	
Middle temporal gyrus	L	5.19	-54	-64	-1	
Middle temporal gyrus	R	5.83	51	-61	5	
Postcentral gyrus	L	5.42	-57	-10	38	
Postcentral gyrus	R	5.21	30	-49	62	
Posterior Cingulate	L	4.96	-9	-37	23	
Posterior Cingulate	R	4.88	3	-49	14	
Precuneus	L	6.36	0	-37	56	
Precuneus	R	6.66	12	-70	41	
Superior occipital gyrus	L	5.51	-18	-91	20	
Superior occipital gyrus	R	5.46	24	-94	11	
Superior temporal gyrus	R	5.16	42	-16	-1	
Supplementary motor area	R	5.16	6	-25	50	
Temporal pole: superior temporal gyrus	L	5.30	-48	11	-7	
Thalamus	L	5.92	-9	-16	2	
Thalamus	R	5.73	6	-19	5	
Inferior frontal gyrus, pars opercularis	R	4.86	51	8	11	357
Inferior frontal gyrus, pars triangularis	R	4.22	57	23	26	
Middle frontal gyrus	R	4.01	39	11	44	
Postcentral gyrus	R	4.52	63	-16	38	
Precentral gyrus	R	5.09	48	8	44	
Superior frontal gyrus, dorsolateral	R	3.90	21	8	59	
Anterior cingulate gyrus	L	3.15	-3	32	26	211
Anterior cingulate gyrus	R	4.32	9	44	23	
Middle cingulate & paracingulate gyri	R	4.50	6	35	35	
Superior frontal gyrus, medial	L	4.33	-3	47	26	
Superior frontal gyrus, medial	R	4.80	3	56	14	
Caudate nucleus	R	3.64	9	14	-4	152
Inferior frontal gyrus, pars orbitalis	R	3.52	24	20	-10	
Insula	R	4.56	42	20	-4	
Lenticular nucleus, Putamen	R	5.04	18	14	-4	

Posterior orbital gyrus	R	3.42	27	29	-13	
Temporal pole: superior temporal gyrus	R	5.30	51	14	-10	
Middle frontal gyrus	L	4.67	-36	50	26	145
Superior frontal gyrus, dorsolateral	L	3.93	-24	23	35	
Middle cingulate & paracingulate gyri	L	3.69	-3	5	35	144
Middle cingulate & paracingulate gyri	R	3.92	6	-1	44	
Supplementary motor area	L	4.71	0	-4	56	
Supplementary motor area	R	4.27	9	11	68	
Inferior parietal gyrus, excluding supramarginal and angular gyri	L	3.77	-24	-55	53	121
Postcentral gyrus	L	4.56	-33	-40	53	
Superior parietal lobule	L	3.98	-27	-49	62	
Anterior cingulate gyrus	L	4.42	0	44	2	98
Superior frontal gyrus, medial orbital	L	3.31	-9	44	-10	
Superior frontal gyrus, medial orbital	R	4.89	6	62	-10	
Inferior temporal gyrus	R	4.72	57	-4	-31	77
Middle temporal gyrus	R	3.98	66	-22	-10	
Superior temporal gyrus	R	3.55	60	-16	-4	
Inferior frontal gyrus, pars triangularis	R	3.16	42	35	5	61
Middle frontal gyrus	R	4.51	42	47	5	
Middle frontal gyrus	R	3.13	36	23	53	52
Superior frontal gyrus, dorsolateral	R	5.30	18	29	56	
Precentral gyrus	L	4.77	-30	-13	65	51
Middle temporal gyrus	L	4.44	-54	-25	-1	48
Superior frontal gyrus, dorsolateral	L	4.95	-21	38	47	43

Note. Table shows one local maxima for each region within each cluster that is separated by more than 8mm. Regions are reported separately for each hemisphere and up to 50 peaks are reported per cluster. Regions were automatically labeled using the BSPMview (http://www.bobspunt.com/bspmview/) implementation of the AAL2 brain parcellation (Rolls, Joliot, & Tzourio-Mazoyer, 2015). Regions not identified by BSPMview (DOI 10.5281/zenodo.168074) with AAL2 were identified based on neuroanatomical examination with the BSPMview implementation of AAL Toolbox (Eickhoff et al., 2005); WFU Pickatlas Individual brain atlases using AAL (Tzourio-Mazoyer et al., 2002), IBASPM71 (Alemán-Gómez, Melie-García, & Valdés-Hernandez, 2006), Talairach Daemon (TD Labels, TD lobes, TD Brodmann areas+) (Lancaster, 1997; Lancaster et al., 1997; Lancaster et al., 2000); Haines Neuroanatomy Atlas (Haines, 2012); and coordinate association in Neurosynth (http://www.neurosynth.org/) (Yarkoni, Poldrack, Nichols, Van Essen, & Wager, 2011). Local maxima are reported with Montreal Neurological Institute (MNI) coordinates x, y, and z in the left-right, anterior-posterior, and inferior-superior dimensions, respectively. Maximal Pseudo-T statistics, and extent in voxels (k) are reported for all significant clusters (cluster defining threshold = 3.01, cluster threshold FWE-corrected $p<0.05$; critical suprathreshold cluster size =38).

Table 3

Functional Connectivity for Neutral Stimuli with Left Amygdala Seed Region

		Psuedo	MNI Coordinates			
Region Label	L/R	t-value	x	y	z	Extent
Amygdala	L	6.639	-24	-4	-13	3469
Angular gyrus	R	4.484	36	-58	47	
Cerebellum crus I	L	5.061	-42	-64	-25	
Cerebellum lobule IV, V	L	4.715	-12	-58	-16	
Cerebellum lobule VI	L	5.693	-21	-64	-19	
Cerebellum lobule VI	R	5.297	24	-61	-19	
Cuneus	L	4.758	-9	-85	32	
Cuneus	R	5.049	15	-82	20	
Fusiform gyrus	L	5.251	-33	-40	-25	
Fusiform gyrus	R	5.587	30	-70	-13	
Hippocampus	L	4.636	-27	-13	-25	
Inferior occipital gyrus	R	4.722	42	-82	-13	
Inferior temporal gyrus	L	4.966	-51	-61	-13	
Inferior temporal gyrus	R	4.592	57	-58	-7	

Lingual gyrus	L	4.593	-21	-55	-13	
Lingual gyrus	R	5.358	27	-64	-4	
Middle cingulate & paracingulate gyri	R	4.466	6	-19	38	
Middle occipital gyrus	L	5.163	-48	-79	14	
Middle occipital gyrus	R	4.876	30	-64	35	
Middle temporal gyrus	L	5.440	-39	-58	20	
Middle temporal gyrus	R	4.648	51	-67	17	
Parahippocampal gyrus	L	7.877	-15	-1	-19	
Postcentral gyrus	R	5.026	12	-43	59	
Posterior orbital gyrus	L	4.618	-21	11	-19	
Precuneus	L	5.473	-12	-64	62	
Precuneus	R	5.703	18	-64	44	
Superior parietal lobule	L	5.312	-21	-70	56	
Superior parietal lobule	R	5.049	27	-58	47	
Vermis lobule VI	R	4.855	3	-61	-25	
Middle cingulate & paracingulate gyri	L	4.336	0	11	41	374
Middle cingulate & paracingulate gyri	R	4.501	6	20	29	
Superior frontal gyrus, dorsolateral	L	3.283	-18	5	65	
Superior frontal gyrus, dorsolateral	R	3.646	15	29	53	
Supplementary motor area	L	6.205	-9	-13	50	
Supplementary motor area	R	4.477	6	2	62	
Inferior frontal gyrus, pars orbitalis	L	4.747	-51	17	-7	236
Insula	L	4.956	-30	8	8	
Lenticular nucleus, Putamen	L	3.550	-24	-1	8	
Rolandic operculum	L	3.492	-54	2	5	
Superior temporal gyrus	L	4.744	-57	2	-13	
Amygdala	R	5.263	27	5	-13	229
Hippocampus	R	3.615	15	-7	-16	
Insula	R	4.889	33	-1	-13	
Middle temporal gyrus	R	3.550	54	-1	-19	
Olfactory cortex	R	3.979	21	11	-19	
Rolandic operculum	R	3.418	48	5	5	
Superior temporal gyrus	R	3.930	57	-13	-10	
Temporal pole: superior temporal gyrus	R	4.152	27	5	-22	
Inferior parietal gyrus, excluding supramarginal and angular gyri	L	4.161	-54	-22	47	171
Postcentral gyrus	L	4.608	-24	-34	59	
Precentral gyrus	L	4.675	-27	-16	68	
Middle temporal gyrus	R	4.882	51	-43	-1	143
Superior temporal gyrus	R	5.206	60	-25	14	
Inferior parietal gyrus, excluding supramarginal and angular gyri	L	3.459	-54	-37	35	126
Rolandic operculum	L	4.191	-45	-22	17	
Superior temporal gyrus	L	4.334	-63	-34	20	
Supramarginal gyrus	L	4.989	-60	-28	26	
Inferior parietal gyrus, excluding supramarginal and angular gyri	R	3.893	42	-49	53	103
Postcentral gyrus	R	4.644	36	-28	53	
Precentral gyrus	R	5.535	27	-22	53	
Middle frontal gyrus	L	4.174	-27	20	53	99
Superior frontal gyrus, dorsolateral	L	4.390	-24	8	68	
Postcentral gyrus	L	5.247	-54	-10	38	98
Precentral gyrus	L	4.338	-45	-1	38	
Lenticular nucleus, Pallidum	R	4.143	15	-4	2	97
Lenticular nucleus, Putamen	R	4.092	27	-10	11	
Thalamus	L	4.314	0	-19	14	
Thalamus	R	4.011	12	-22	11	

Inferior frontal gyrus, pars triangularis	R	4.466	33	29	2	80
Middle frontal gyrus	R	3.243	48	50	-1	
Basilar Pons	R	3.141	12	-13	-28	73
Hippocampus	R	4.663	21	-19	-10	
Parahippocampal gyrus	R	5.223	21	-16	-25	
Postcentral gyrus	R	4.444	63	-10	20	65
Precentral gyrus	R	4.233	60	8	20	
Rolandic operculum	R	4.276	60	-1	14	
Superior frontal gyrus, dorsolateral	R	4.538	24	14	56	54

Note. Table shows one local maxima for each region within each cluster that is separated by more than 8mm. Regions are reported separately for each hemisphere and up to 50 peaks are reported per cluster. Regions were automatically labeled using the BSPMview (http://www.bobspunt.com/bspmview/) implementation of the AAL2 brain parcellation (Rolls, Joliot, & Tzourio-Mazoyer, 2015). Regions not identified by BSPMview (DOI 10.5281/zenodo.168074) with AAL2 were identified based on neuroanatomical examination with the BSPMview implementation of AAL Toolbox (Eickhoff et al., 2005); WFU Pickatlas Individual brain atlases using AAL (Tzourio-Mazoyer et al., 2002), IBASPM71 (Alemán-Gómez, Melie-García, & Valdés-Hernandez, 2006), Talairach Daemon (TD Labels, TD lobes, TD Brodmann areas+) (Lancaster, 1997; Lancaster et al., 1997; Lancaster et al., 2000); Haines Neuroanatomy Atlas (Haines, 2012); and coordinate association in Neurosynth (http://www.neurosynth.org/) (Yarkoni, Poldrack, Nichols, Van Essen, & Wager, 2011). Local maxima are reported with Montreal Neurological Institute (MNI) coordinates x, y, and z in the left-right, anterior-posterior, and inferior-superior dimensions, respectively. Maximal Pseudo-T statistics, and extent in voxels (k) are reported for all significant clusters (cluster defining threshold = 3.01, cluster threshold FWE-corrected $p<0.05$; critical suprathreshold cluster size =40).

Table 4

Functional Connectivity for Neutral Stimuli with Right Amygdala Seed Region

		Psuedo	MNI Coordinates			
Region Label	L/R	t-value	x	y	z	Extent
Amygdala	L	4.286	-12	-4	-10	3421
Calcarine fissure and surrounding cortex	L	5.013	3	-88	8	
Calcarine fissure and surrounding cortex	R	5.353	15	-61	17	
Caudate nucleus	L	4.710	-9	11	-1	
Cerebellum crus II	L	4.363	-6	-73	-31	
Cerebellum lobule IV, V	L	4.522	-6	-49	-1	
Cerebellum lobule VI	L	4.571	-27	-61	-22	
Cerebellum lobule VI	R	5.064	30	-61	-22	
Cuneus	L	4.815	0	-79	17	
Cuneus	R	4.954	12	-73	32	
Fusiform gyrus	R	5.830	30	-73	-16	
Hippocampus	L	4.928	-24	-16	-19	
Inferior temporal gyrus	R	4.484	57	-58	-7	
Lingual gyrus	L	4.285	-9	-61	-1	
Lingual gyrus	R	4.373	21	-70	-1	
Middle cingulate & paracingulate gyri	L	4.482	0	-25	41	
Middle cingulate & paracingulate gyri	R	5.367	6	-25	47	
Middle occipital gyrus	L	4.476	-12	-94	-1	
Middle occipital gyrus	R	5.077	42	-76	-1	
Middle temporal gyrus	R	4.727	51	-61	2	
Posterior cingulate gyrus	L	4.463	-6	-43	5	
Posterior cingulate gyrus	R	4.806	6	-43	23	
Precuneus	L	5.916	0	-40	56	
Precuneus	R	5.752	6	-61	23	
Superior occipital gyrus	L	5.219	-18	-91	20	
Superior occipital gyrus	R	4.842	24	-94	11	
Superior temporal gyrus	R	4.505	48	-28	-4	
Thalamus	L	5.573	0	-7	11	
Thalamus	R	4.983	9	-1	8	

Amygdala	R	8.640	24	-1	-16	508
Amygdala	R	4.173	15	-10	-16	
Caudate nucleus	R	3.567	18	17	-4	
Fusiform gyrus	R	4.659	39	-10	-31	
Heschl's gyrus	R	5.178	45	-16	11	
Hippocampus	R	4.708	21	-19	-13	
Inferior frontal gyrus, pars orbitalis	R	3.839	24	20	-10	
Inferior temporal gyrus	R	4.000	48	2	-34	
Lenticular nucleus, Pallidum	R	3.189	30	-10	-7	
Lenticular nucleus, Putamen	R	4.326	30	-16	-1	
Midbrain	R	4.919	12	-28	-22	
Parahippocampal gyrus	R	3.965	21	-19	-25	
Posterior orbital gyrus	R	3.369	27	32	-16	
Superior temporal gyrus	R	4.713	42	-16	-1	
Inferior temporal gyrus	L	4.017	-51	-64	-13	479
Middle occipital gyrus	L	4.844	-33	-85	2	
Middle temporal gyrus	L	4.828	-60	-55	-1	
Postcentral gyrus	L	4.694	-57	-10	38	
Superior temporal gyrus	L	5.539	-54	-49	17	
Supramarginal gyrus	L	4.832	-57	-40	32	
Inferior frontal gyrus, pars opercularis	L	4.654	-54	5	5	245
Inferior frontal gyrus, pars orbitalis	L	4.172	-39	20	-4	
Insula	L	4.451	-30	17	5	
Lenticular nucleus, Putamen	L	4.868	-27	-13	5	
Precentral gyrus	L	4.392	-51	-1	20	
Superior temporal gyrus	L	3.976	-57	-1	-1	
Temporal pole: superior temporal gyrus	L	4.672	-51	11	-7	
Middle temporal gyrus	R	5.986	66	-40	8	141
Superior temporal gyrus	R	4.381	69	-37	17	
Supramarginal gyrus	R	4.479	54	-31	35	
Anterior cingulate gyrus	L	3.703	-3	38	23	116
Anterior cingulate gyrus	R	4.369	6	47	20	
Superior frontal gyrus, medial	L	4.286	-3	47	26	
Superior frontal gyrus, medial	R	4.139	3	56	14	
Inferior frontal gyrus, pars opercularis	R	5.761	54	14	38	115
Inferior frontal gyrus, pars triangularis	R	3.232	45	11	23	
Middle frontal gyrus	R	3.607	39	11	44	
Precentral gyrus	R	4.534	48	8	44	
Anterior cingulate gyrus	L	3.846	-12	47	-1	113
Anterior orbital gyrus	L	3.157	-12	53	-13	
Superior frontal gyrus, medial orbital	L	3.819	-9	35	-13	
Superior frontal gyrus, medial orbital	R	4.648	6	62	-13	
Postcentral gyrus	R	4.181	63	-16	38	97
Precentral gyrus	R	4.146	57	-10	47	
Inferior parietal gyrus, excluding supramarginal and angular gyri	L	3.231	-24	-55	53	79
Postcentral gyrus	L	4.121	-33	-37	56	
Superior parietal lobule	L	4.061	-27	-49	59	
Middle frontal gyrus	L	4.460	-33	44	29	63
Middle frontal gyrus	R	3.603	36	17	56	58
Superior frontal gyrus, dorsolateral	R	4.231	30	29	56	
Thalamus	R	5.406	6	-19	5	
Insula	R	4.270	42	20	-4	56
Temporal pole: superior temporal gyrus	R	4.905	51	14	-10	
Middle cingulate & paracingulate gyri	R	3.734	6	-1	44	41

Middle temporal gyrus	R	5.152	60	-1	-31
Superior temporal gyrus	R	3.567	63	2	-13
Supplementary motor area	L	4.141	-3	-4	56
Supplementary motor area	R	3.228	3	8	53

Note. Table shows one local maxima for each region within each cluster that is separated by more than 8mm. Regions are reported separately for each hemisphere and up to 50 peaks are reported per cluster. Regions were automatically labeled using the BSPMview (http://www.bobspunt.com/bspmview/) implementation of the AAL2 brain parcellation (Rolls, Joliot, & Tzourio-Mazoyer, 2015). Regions not identified by BSPMview (DOI 10.5281/zenodo.168074) with AAL2 were identified based on neuroanatomical examination with the BSPMview implementation of AAL Toolbox (Eickhoff et al., 2005); WFU Pickatlas Individual brain atlases using AAL (Tzourio-Mazoyer et al., 2002), IBASPM71 (Alemán-Gómez, Melie-García, & Valdés-Hernandez, 2006), Talairach Daemon (TD Labels, TD lobes, TD Brodmann areas+) (Lancaster, 1997; Lancaster et al., 1997; Lancaster et al., 2000); Haines Neuroanatomy Atlas (Haines, 2012); and coordinate association in Neurosynth (http://www.neurosynth.org/) (Yarkoni, Poldrack, Nichols, Van Essen, & Wager, 2011). Local maxima are reported with Montreal Neurological Institute (MNI) coordinates x, y, and z in the left-right, anterior-posterior, and inferior-superior dimensions, respectively. Maximal Pseudo-T statistics, and extent in voxels (k) are reported for all significant clusters (cluster defining threshold = 3.01, cluster threshold FWE-corrected $p<0.05$; critical suprathreshold cluster size =36).

Table 5

Functional Connectivity for Emotional Stimuli (Positive and Negative) with Left Amygdala Seed Region

			Pseudo	MNI Coordinates		
Region Label	L/R	Extent	t-value	x	y	z
Amygdala	L	7387	8.571	-18	-4	-19
Angular gyrus	L		5.262	-39	-61	23
Calcarine fissure and surrounding cortex	L		5.533	3	-82	-4
Cerebellum crus I	L		5.248	-42	-64	-25
Cerebellum lobule IV, V	L		4.960	-6	-64	-7
Cerebellum lobule VI	L		5.803	-33	-52	-31
Cerebellum lobule VI	R		5.501	9	-76	-19
Cuneus	L		5.112	-9	-88	32
Fusiform gyrus	L		5.236	-24	-73	-7
Fusiform gyrus	R		6.565	27	-70	-13
Inferior occipital gyrus	L		5.164	-45	-64	-13
Inferior temporal gyrus	R		5.703	60	-61	-4
Insula	L		5.433	-42	2	2
Lingual gyrus	L		5.200	-6	-82	-7
Lingual gyrus	R		5.385	27	-64	-4
Middle cingulate & paracingulate gyri	L		4.884	0	-22	41
Middle cingulate & paracingulate gyri	R		5.753	3	23	29
Middle occipital gyrus	L		5.494	-42	-76	-1
Middle occipital gyrus	R		5.134	30	-64	32
Middle temporal gyrus	L		6.071	-54	-55	14
Middle temporal gyrus	R		6.204	51	-43	2
Precuneus	L		5.498	0	-55	14
Precuneus	R		5.565	18	-64	44
Rolandic operculum	L		5.081	-39	-28	20
Superior frontal gyrus, dorsolateral	R		5.759	39	-4	62
Superior parietal lobule	L		5.333	-18	-76	50
Superior temporal gyrus	L		4.884	-63	-31	14
Superior temporal gyrus	R		5.073	60	-25	14
Supplementary motor area	L		5.372	0	2	53
Supramarginal gyrus	L		4.976	-57	-25	23
Amygdala	R	557	5.759	27	5	-16
Gyrus rectus	R		3.507	21	14	-13
Hippocampus	R		5.000	27	-34	-4
Insula	R		4.558	39	5	-16

Lenticular nucleus, Pallidum	R		4.029	15	-4	-1
Lenticular nucleus, Putamen	R		4.723	30	-13	8
Midbrain	R		4.437	9	-28	-22
Olfactory cortex	R		4.226	18	8	-19
Parahippocampal gyrus	R		4.616	24	-13	-28
Thalamus	L		4.505	-3	-19	11
Thalamus	R		4.548	12	-19	5
Anterior cingulate gyrus	L	174	3.848	0	44	2
Gyrus rectus	L		4.100	-6	44	-19
Superior frontal gyrus, dorsolateral	L		4.606	-12	65	17
Superior frontal gyrus, medial	L		5.542	0	65	20
Superior frontal gyrus, medial	R		4.207	3	56	14
Superior frontal gyrus, medial orbital	L		4.437	-6	44	-10
Inferior parietal gyrus, excluding supramarginal and angular gyri	L	156	3.537	-51	-37	53
Postcentral gyrus	L		4.361	-33	-40	65
Precentral gyrus	L		4.834	-30	-16	68
Inferior frontal gyrus, pars triangularis	L	123	3.792	-48	32	23
Middle frontal gyrus	L		4.676	-42	38	23
Rolandic operculum	L	87	4.137	-54	-7	8
Superior temporal gyrus	L		5.064	-60	-1	2
Inferior frontal gyrus, pars orbitalis	R	84	4.110	57	29	-4
Insula	R		3.958	45	20	-10
Lateral orbital gyrus	R		3.342	48	35	-16
Temporal pole: superior temporal gyrus	R		4.662	45	17	-22
Middle temporal gyrus	R	83	4.306	57	-22	-10
Superior temporal gyrus	R		4.416	57	-13	-10
Temporal pole: middle temporal gyrus	R		3.256	57	8	-19
Heschl's gyrus	R	79	3.254	63	-4	5
Insula	R		3.823	48	-7	-1
Rolandic operculum	R		3.917	57	2	8
Superior temporal gyrus	R		4.052	54	-1	-1
Temporal pole: superior temporal gyrus	R		4.244	63	8	-1
Superior frontal gyrus, dorsolateral	R	69	4.483	27	47	41
Superior frontal gyrus, medial	R		4.801	12	50	47

Note. Table shows one local maxima for each region within each cluster that is separated by more than 8mm. Regions are reported separately for each hemisphere and up to 50 peaks are reported per cluster. Regions were automatically labeled using the BSPMview (http://www.bobspunt.com/bspmview/) implementation of the AAL2 brain parcellation (Rolls, Joliot, & Tzourio-Mazoyer, 2015). Regions not identified by BSPMview (DOI 10.5281/zenodo.168074) with AAL2 were identified based on neuroanatomical examination with the BSPMview implementation of AAL Toolbox (Eickhoff et al., 2005); WFU Pickatlas Individual brain atlases using AAL (Tzourio-Mazoyer et al., 2002), IBASPM71 (Alemán-Gómez, Melie-García, & Valdés-Hernandez, 2006), Talairach Daemon (TD Labels, TD lobes, TD Brodmann areas+) (Lancaster, 1997; Lancaster et al., 1997; Lancaster et al., 2000); Haines Neuroanatomy Atlas (Haines, 2012); and coordinate association in Neurosynth (http://www.neurosynth.org/) (Yarkoni, Poldrack, Nichols, Van Essen, & Wager, 2011). Local maxima are reported with Montreal Neurological Institute (MNI) coordinates x, y, and z in the left-right, anterior-posterior, and inferior-superior dimensions, respectively. Maximal Pseudo-T statistics, and extent in voxels (k) are reported for all significant clusters (cluster defining threshold = 3.01, cluster threshold FWE-corrected $p<0.05$; critical suprathreshold cluster size =39).

Table 6

Functional Connectivity for Emotional Stimuli (Positive and Negative) With Right Amygdala Seed Region

		Pseudo	MNI Coordinates			
Region Label	L/R	t-value	x	y	z	Extent
Amygdala	R	10.135	30	-1	-19	5487
Calcarine fissure and surrounding cortex	L	5.451	-21	-64	8	
Calcarine fissure and surrounding cortex	R	5.333	6	-82	-1	

Cerebellum lobule VI	R	5.844	21	-79	-16	
Cuneus	L	4.815	0	-79	20	
Fusiform gyrus	L	5.283	-30	-67	-19	
Fusiform gyrus	R	6.823	30	-73	-16	
Heschl's gyrus	R	4.897	42	-19	11	
Hippocampus	R	5.473	21	-16	-16	
Inferior temporal gyrus	R	4.661	60	-64	-4	
Lingual gyrus	L	5.368	-9	-58	-1	
Lingual gyrus	R	4.974	12	-70	-10	
Middle occipital gyrus	L	5.717	-30	-85	2	
Middle occipital gyrus	R	5.106	45	-76	-1	
Middle temporal gyrus	L	5.017	-51	-67	2	
Middle temporal gyrus	R	5.796	51	-64	5	
Postcentral gyrus	R	5.607	30	-49	62	
Posterior cingulate	L	5.219	-9	-37	23	
Precuneus	L	5.582	0	-37	56	
Precuneus	R	6.421	9	-70	41	
Superior occipital gyrus	L	5.398	-18	-82	38	
Superior occipital gyrus	R	5.364	24	-94	14	
Superior parietal lobule	R	4.898	18	-58	53	
Superior temporal gyrus	R	4.873	54	-25	8	
Supplementary motor area	R	5.157	6	-25	50	
Temporal pole: superior temporal gyrus	R	5.635	36	5	-25	
Vermis lobule VII	L	4.619	-3	-70	-28	
Amygdala	L	4.541	-21	-4	-13	1274
Caudate nucleus	L	4.735	-12	11	-1	
Caudate nucleus	R	4.681	9	-1	8	
Fusiform gyrus	L	4.004	-27	-34	-19	
Heschl's gyrus	L	4.212	-30	-25	5	
Hippocampus	L	4.842	-24	-19	-19	
Inferior frontal gyrus, pars opercularis	L	4.943	-54	8	14	
Inferior frontal gyrus, pars orbitalis	L	4.568	-39	17	-13	
Inferior frontal gyrus, pars triangularis	L	3.758	-45	20	20	
Insula	L	4.785	-42	2	-1	
Lenticular nucleus, Putamen	L	5.632	-27	-10	-1	
Lenticular nucleus, Putamen	R	3.855	27	5	8	
Midbrain	L	3.880	-12	-28	-7	
Middle temporal gyrus	L	4.352	-57	-7	-10	
Postcentral gyrus	L	5.400	-57	-10	38	
Posterior orbital gyrus	L	4.663	-33	17	-19	
Precentral gyrus	L	5.129	-54	5	29	
Superior temporal gyrus	L	4.385	-54	-1	-4	
Supramarginal gyrus	L	4.000	-63	-25	26	
Temporal pole: superior temporal gyrus	L	5.224	-48	11	-7	
Thalamus	L	5.727	-9	-16	2	
Thalamus	R	5.684	6	-19	5	
Middle cingulate & paracingulate gyri	L	4.130	-3	5	38	220
Middle cingulate & paracingulate gyri	R	3.350	6	2	38	
Superior frontal gyrus, dorsolateral	L	5.033	-21	38	47	
Superior frontal gyrus, medial	L	3.391	-3	26	50	
Supplementary motor area	L	4.774	0	-4	56	
Supplementary motor area	R	5.404	3	-7	71	
Anterior cingulate gyrus	R	3.961	9	44	23	178
Middle cingulate & paracingulate gyri	R	4.437	6	32	35	

Superior frontal gyrus, medial	L	4.509	3	65	23	
Superior frontal gyrus, medial	R	4.830	3	56	14	
Middle frontal gyrus	R	4.622	36	-1	62	165
Middle frontal gyrus	R	3.578	45	-4	56	
Postcentral gyrus	R	4.120	63	-16	38	
Precentral gyrus	R	4.727	45	-19	62	
Superior frontal gyrus, dorsolateral	R	3.751	24	8	56	
Inferior frontal gyrus, pars triangularis	L	3.539	-42	32	23	144
Middle frontal gyrus	L	4.628	-36	44	29	
Superior frontal gyrus, dorsolateral	L	4.217	-24	23	35	
Inferior frontal gyrus, pars opercularis	R	4.025	48	11	35	129
Inferior frontal gyrus, pars triangularis	R	3.977	57	23	26	
Insula	R	4.460	42	20	-4	
Lenticular nucleus, Putamen	R	5.064	18	14	-4	
Precentral gyrus	R	4.931	48	8	44	
Temporal pole: superior temporal gyrus	R	5.002	51	14	-10	
Middle temporal gyrus	L	4.567	-54	-25	-1	76
Superior temporal gyrus	L	3.622	-60	-31	11	
Supramarginal gyrus	L	4.444	-63	-40	29	61
Postcentral gyrus	L	4.274	-36	-34	50	60
Superior parietal lobule	L	4.009	-39	-49	62	57
Anterior cingulate gyrus	L	4.258	0	44	2	53
Superior frontal gyrus, medial orbital	L	3.578	0	53	-4	
Cerebellum lobule IV, V	R	4.132	24	-31	-28	46
Fusiform gyrus	R	4.440	24	-37	-19	

Note. Table shows one local maxima for each region within each cluster that is separated by more than 8mm. Regions are reported separately for each hemisphere and up to 50 peaks are reported per cluster. Regions were automatically labeled using the BSPMview (http://www.bobspunt.com/bspmview/) implementation of the AAL2 brain parcellation (Rolls, Joliot, & Tzourio-Mazoyer, 2015). Regions not identified by BSPMview (DOI 10.5281/zenodo.168074) with AAL2 were identified based on neuroanatomical examination with the BSPMview implementation of AAL Toolbox (Eickhoff et al., 2005); WFU Pickatlas Individual brain atlases using AAL (Tzourio-Mazoyer et al., 2002), IBASPM71 (Alemán-Gómez, Melie-García, & Valdés-Hernandez, 2006), Talairach Daemon (TD Labels, TD lobes, TD Brodmann areas+) (Lancaster, 1997; Lancaster et al., 1997; Lancaster et al., 2000); Haines Neuroanatomy Atlas (Haines, 2012); and coordinate association in Neurosynth (http://www.neurosynth.org/) (Yarkoni, Poldrack, Nichols, Van Essen, & Wager, 2011). Local maxima are reported with Montreal Neurological Institute (MNI) coordinates x, y, and z in the left-right, anterior-posterior, and inferior-superior dimensions, respectively. Maximal Pseudo-T statistics, and extent in voxels (k) are reported for all significant clusters (cluster defining threshold = 3.01, cluster threshold FWE-corrected $p<0.05$; critical suprathreshold cluster size =34).

Table 7

Functional Connectivity for Negative Stimuli With Left Amygdala Seed Region

		Pseudo	MNI Coordinates			
Region Label	L/R	t-value	x	y	z	Extent
Amygdala	L	8.974	-21	-1	-22	3788
Calcarine fissure and surrounding cortex	L	5.395	3	-82	-4	
Cerebellum crus I	L	5.392	-39	-61	-28	
Cerebellum lobule IV, V	L	4.785	-15	-52	-28	
Cerebellum lobule VI	L	5.705	-15	-73	-22	
Cerebellum lobule VI	R	5.911	9	-76	-19	
Fusiform gyrus	L	4.720	-24	-73	-7	
Fusiform gyrus	R	5.564	30	-73	-13	
Inferior occipital gyrus	L	4.782	-27	-91	-10	
Inferior temporal gyrus	R	4.982	45	-49	-25	
Lingual gyrus	L	5.201	-12	-61	-7	
Lingual gyrus	R	6.091	27	-64	-4	
Middle occipital gyrus	L	4.880	-42	-76	-1	

Middle occipital gyrus	R	5.272	30	-64	32	
Middle temporal gyrus	L	4.663	-48	-73	17	
Olfactory cortex	L	4.961	-9	2	-16	
Parahippocampal gyrus	L	4.390	-18	-37	-13	
Posterior orbital gyrus	L	4.533	-27	14	-22	
Precuneus	L	5.439	0	-55	14	
Precuneus	R	4.662	9	-52	62	
Superior parietal lobule	L	5.387	-21	-52	41	
Temporal pole: superior temporal gyrus	L	4.690	-45	20	-25	
Vermis lobule VI	R	4.556	3	-64	-22	
Anterior cingulate gyrus	L	3.725	-6	20	29	316
Middle cingulate & paracingulate gyri	L	4.724	-12	-19	38	
Middle cingulate & paracingulate gyri	R	4.921	3	23	29	
Superior frontal gyrus, dorsolateral	R	3.572	18	-10	53	
Supplementary motor area	L	4.830	-6	-10	56	
Supplementary motor area	R	4.942	3	-7	71	
Amygdala	R	4.633	24	-1	-10	200
Hippocampus	R	4.323	21	-16	-10	
Insula	R	3.780	39	5	-16	
Lenticular nucleus, Pallidum	R	3.337	15	-4	-1	
Lenticular nucleus, Putamen	R	5.097	27	8	-13	
Midbrain	R	4.479	6	-10	-10	
Olfactory cortex	R	4.363	18	8	-19	
Inferior parietal gyrus, excluding supramarginal and angular gyri	R	3.283	42	-46	53	196
Postcentral gyrus	R	4.656	30	-34	62	
Precentral gyrus	R	4.707	30	-22	59	
Superior frontal gyrus, dorsolateral	R	6.094	39	-4	62	
Superior parietal lobule	R	3.584	39	-46	62	
Supplementary motor area	R	3.402	15	-19	62	
Middle temporal gyrus	R	6.093	51	-43	-1	194
Postcentral gyrus	R	3.895	45	-22	32	
Rolandic operculum	R	4.600	45	-22	23	
Superior temporal gyrus	R	4.545	63	-25	14	
Supramarginal gyrus	R	3.719	63	-40	23	
Angular gyrus	L	4.315	-39	-61	23	151
Middle temporal gyrus	L	5.310	-54	-52	14	
Middle temporal gyrus	L	3.414	-45	-64	17	
Superior temporal gyrus	L	4.729	-42	-43	11	
Supramarginal gyrus	L	3.458	-60	-52	23	
Postcentral gyrus	L	4.758	-36	-40	65	105
Precentral gyrus	L	4.349	-30	-16	68	
Inferior frontal gyrus, pars triangularis	L	3.537	-51	20	17	76
Middle frontal gyrus	L	4.162	-42	38	23	
Inferior frontal gyrus, pars orbitalis	R	4.101	57	32	-4	61
Posterior orbital gyrus	R	3.415	45	23	-16	
Temporal pole: superior temporal gyrus	R	3.963	54	20	-10	
Caudate nucleus	L	3.766	-9	11	2	50
Lenticular nucleus, Putamen	L	4.376	-27	8	2	

Note. Table shows one local maxima for each region within each cluster that is separated by more than 8mm. Regions are reported separately for each hemisphere and up to 50 peaks are reported per cluster. Regions were automatically labeled using the BSPMview (http://www.bobspunt.com/bspmview/) implementation of the AAL2 brain parcellation (Rolls, Joliot, & Tzourio-Mazoyer, 2015). Regions not identified by BSPMview (DOI 10.5281/zenodo.168074) with AAL2 were identified based on neuroanatomical examination with the BSPMview implementation of AAL Toolbox (Eickhoff et al., 2005); WFU Pickatlas Individual brain atlases using AAL (Tzourio-Mazoyer et al., 2002), IBASPM71 (Alemán-Gómez, Melie-García, & Valdés-

Hernandez, 2006), Talairach Daemon (TD Labels, TD lobes, TD Brodmann areas+) (Lancaster, 1997; Lancaster et al., 1997; Lancaster et al., 2000); Haines Neuroanatomy Atlas (Haines, 2012); and coordinate association in Neurosynth (http://www.neurosynth.org/) (Yarkoni, Poldrack, Nichols, Van Essen, & Wager, 2011). Local maxima are reported with Montreal Neurological Institute (MNI) coordinates x, y, and z in the left-right, anterior-posterior, and inferior-superior dimensions, respectively. Maximal Pseudo-T statistics, and extent in voxels (k) are reported for all significant clusters (cluster defining threshold = 3.01, cluster threshold FWE-corrected $p<0.05$; critical suprathreshold cluster size =39).

Table 8

Functional Connectivity for Negative Stimuli With Right Amygdala Seed Region

		Pseudo	MNI Coordinates			
Region Label	L/R	t-value	x	y	z	Extent
Calcarine fissure and surrounding cortex	L	4.923	-15	-82	8	3383
Calcarine fissure and surrounding cortex	R	5.775	6	-82	-1	
Cerebellum crus I	R	4.601	36	-67	-28	
Cerebellum lobule VI	L	4.362	-27	-61	-22	
Cerebellum lobule VI	R	5.254	24	-64	-16	
Cuneus	L	4.767	0	-79	20	
Cuneus	R	4.488	15	-100	5	
Fusiform gyrus	L	4.838	-30	-67	-16	
Fusiform gyrus	R	5.424	30	-73	-16	
Lingual gyrus	L	5.042	-12	-58	-1	
Lingual gyrus	R	4.786	12	-70	-13	
Middle occipital gyrus	L	6.394	-24	-100	5	
Middle occipital gyrus	R	4.980	27	-91	5	
Middle temporal gyrus	R	4.786	51	-61	5	
Postcentral gyrus	R	4.794	30	-49	62	
Posterior cingulate gyrus	R	4.306	6	-43	23	
Precuneus	L	4.563	0	-37	56	
Precuneus	R	5.457	12	-55	29	
Superior occipital gyrus	L	5.291	-18	-82	38	
Superior occipital gyrus	R	5.553	24	-97	14	
Superior parietal lobule	R	4.415	39	-49	62	
Amygdala	R	10.200	24	-1	-16	299
Hippocampus	R	4.947	21	-16	-16	
Lenticular nucleus, Pallidum	R	3.602	21	-4	-4	
Lenticular nucleus, Putamen	R	4.158	33	-4	2	
Parahippocampal gyrus	R	4.995	30	5	-31	
Posterior orbital gyrus	R	4.500	27	14	-22	
Temporal pole: middle temporal gyrus	R	4.269	36	11	-37	
Inferior frontal gyrus, pars opercularis	L	3.934	-54	5	5	247
Insula	L	4.565	-27	17	-19	
Middle temporal gyrus	L	4.697	-57	-34	-4	
Superior temporal gyrus	L	4.425	-51	-7	-7	
Temporal pole: superior temporal gyrus	L	4.455	-51	14	-7	
Heschl's gyrus	R	5.219	45	-19	11	155
Insula	R	4.081	45	-10	11	
Lenticular nucleus, Putamen	R	4.464	30	-16	-1	
Middle temporal gyrus	R	3.209	54	-40	-4	
Rolandic operculum	R	4.076	63	-19	14	
Superior temporal gyrus	R	4.952	48	-31	-4	
Amygdala	L	3.982	-21	-4	-13	106
Fusiform gyrus	L	3.829	-24	-37	-22	
Hippocampus	L	4.339	-27	-22	-16	
Lenticular nucleus, Putamen	L	3.306	-24	11	-10	

Midbrain	L	3.823	0	-22	-19	
Olfactory cortex	L	3.636	-18	5	-16	
Caudate nucleus	L	4.223	-9	-1	8	91
Caudate nucleus	R	3.561	3	-1	14	
Lenticular nucleus, Putamen	L	3.974	-15	8	2	
Thalamus	L	4.064	-3	-16	11	
Inferior frontal gyrus, pars triangularis	L	4.577	-42	32	23	85
Middle frontal gyrus	L	4.854	-39	47	29	
Superior frontal gyrus, medial	L	3.713	-3	50	17	81
Caudate nucleus	R	5.094	21	-16	20	79
Thalamus	R	5.267	6	-19	5	
Postcentral gyrus	R	3.425	63	-13	32	69
Middle frontal gyrus	L	4.132	-63	-19	38	61
Postcentral gyrus	L	5.696	-57	-10	38	
Inferior frontal gyrus, pars opercularis	R	3.197	48	11	35	59
Middle frontal gyrus	R	3.490	51	14	50	
Precentral gyrus	R	4.866	54	5	44	
Middle cingulate & paracingulate gyri	L	3.699	-3	-25	44	56
Middle cingulate & paracingulate gyri	R	4.828	9	-25	47	
Inferior temporal gyrus	L	3.680	-45	-61	-10	55
Middle temporal gyrus	L	4.249	-57	-58	14	
Superior temporal gyrus	L	4.982	-57	-49	17	
Inferior frontal gyrus, pars opercularis	L	3.423	-57	14	23	52
Precentral gyrus	L	4.764	-54	2	26	
Caudate nucleus	R	4.862	9	-1	8	50
Lenticular nucleus, Putamen	R	4.879	21	14	-1	
Fusiform gyrus	L	3.499	-33	-52	-7	49
Middle temporal gyrus	L	4.451	-42	-46	11	
Superior temporal gyrus	L	4.536	-45	-37	11	
Anterior cingulate gyrus	R	3.585	9	44	26	48
Middle cingulate & paracingulate gyri	R	4.122	9	38	32	
Heschl's gyrus	L	3.431	-33	-25	8	47
Insula	L	3.890	-36	-7	-4	
Lenticular nucleus, Putamen	L	5.096	-27	-16	2	
Inferior parietal gyrus, excluding supramarginal and angular gyri	L	3.217	-45	-28	47	45
Postcentral gyrus	L	4.268	-30	-37	71	
Middle frontal gyrus	L	4.922	-24	29	56	41
Superior frontal gyrus, dorsolateral	L	4.746	-21	38	47	
Insula	R	4.118	39	17	-4	39
Middle frontal gyrus	R	3.302	39	5	59	
Precentral gyrus	R	3.813	45	-19	62	
Superior frontal gyrus, dorsolateral	R	3.833	36	-4	62	
Temporal pole: superior temporal gyrus	L	5.125	48	14	-10	
Supplementary motor area	L	3.809	0	14	56	38
Superior temporal gyrus	R	5.091	66	-37	8	37

Note. Table shows one local maxima for each region within each cluster that is separated by more than 8mm. Regions are reported separately for each hemisphere and up to 50 peaks are reported per cluster. Regions were automatically labeled using the BSPMview (http://www.bobspunt.com/bspmview/) implementation of the AAL2 brain parcellation (Rolls, Joliot, & Tzourio-Mazoyer, 2015). Regions not identified by BSPMview (DOI 10.5281/zenodo.168074) with AAL2 were identified based on neuroanatomical examination with the BSPMview implementation of AAL Toolbox (Eickhoff et al., 2005); WFU Pickatlas Individual brain atlases using AAL (Tzourio-Mazoyer et al., 2002), IBASPM71 (Alemán-Gómez, Melie-García, & Valdés-Hernandez, 2006), Talairach Daemon (TD Labels, TD lobes, TD Brodmann areas+) (Lancaster, 1997; Lancaster et al., 1997; Lancaster et al., 2000); Haines Neuroanatomy Atlas (Haines, 2012); and coordinate association in Neurosynth (http://www.neurosynth.org/) (Yarkoni, Poldrack, Nichols, Van Essen, & Wager, 2011). Local maxima are reported with Montreal Neurological Institute (MNI) coordinates x, y, and z in the left-right, anterior-posterior, and inferior-superior

dimensions, respectively. Maximal Pseudo-T statistics, and extent in voxels (k) are reported for all significant clusters (cluster defining threshold = 3.01, cluster threshold FWE-corrected p<0.05; critical suprathreshold cluster size =31).

Table 9

Functional Connectivity for Positive Stimuli with Left Amygdala Seed Region

		Pseudo	MNI Coordinates			
Region Label	L/R	t-value	x	y	z	Extent
Amygdala	L	8.220	-24	-1	-19	5431
Angular gyrus	L	5.198	-39	-61	23	
Calcarine fissure and surrounding cortex	L	5.020	3	-82	-4	
Cerebellum lobule IV, V	L	4.729	-6	-64	-7	
Cerebellum lobule VI	L	5.323	-33	-52	-31	
Cerebellum lobule VI	R	5.267	21	-67	-19	
Cuneus	L	5.077	-9	-85	32	
Fusiform gyrus	L	5.685	-36	-64	-13	
Fusiform gyrus	R	5.857	27	-70	-13	
Hippocampus	L	4.924	-21	-16	-13	
Inferior occipital gyrus	L	5.219	-48	-61	-16	
Inferior occipital gyrus	R	5.019	30	-82	-10	
Inferior temporal gyrus	R	5.303	60	-61	-4	
Insula	L	5.699	-42	2	2	
Lenticular nucleus, Pallidum	L	4.780	-12	5	-1	
Lingual gyrus	L	5.108	-9	-79	-7	
Lingual gyrus	R	5.361	15	-82	-13	
Middle cingulate & paracingulate gyri	L	4.817	0	-22	41	
Middle cingulate & paracingulate gyri	R	5.048	3	23	29	
Middle occipital gyrus	L	5.662	-42	-76	2	
Middle occipital gyrus	R	4.914	33	-76	32	
Middle temporal gyrus	L	5.650	-51	-52	14	
Middle temporal gyrus	R	5.721	51	-43	2	
Postcentral gyrus	R	4.745	15	-43	59	
Posterior cingulate gyrus	L	4.793	0	-52	14	
Precuneus	L	4.687	-12	-61	53	
Precuneus	R	5.959	18	-64	44	
Superior temporal gyrus	R	5.307	60	-25	14	
Supplementary motor area	L	5.960	-9	-13	47	
Supplementary motor area	R	5.265	9	-1	50	
Temporal pole: superior temporal gyrus	L	5.539	-57	11	-10	
Amygdala	R	5.777	33	-1	-13	460
Caudate nuclues	L	3.612	0	2	17	
Heschl's gyrus	R	3.601	45	-22	8	
Hippocampus	R	4.627	15	-10	-16	
Insula	R	4.594	39	5	-16	
Lenticular nucleus, Pallidum	R	3.442	12	-1	-7	
Lenticular nucleus, Putamen	R	4.616	30	-13	8	
Midbrain	R	4.589	9	-19	-7	
Middle temporal gyrus	R	3.515	51	-4	-19	
Olfactory cortex	R	4.379	18	11	-19	
Parahippocampal gyrus	R	4.407	24	-13	-28	
Superior temporal gyrus	R	3.646	42	-19	-1	
Thalamus	L	3.360	-3	-7	5	
Thalamus	R	4.227	12	-19	5	
Heschl's gyrus	L	3.680	-39	-25	11	191
Inferior parietal gyrus, excluding supramarginal and angular gyri	L	3.690	-33	-31	35	

Insula	L	3.773	-30	-25	14	
Postcentral gyrus	L	4.213	-60	-13	29	
Precentral gyrus	L	4.930	-54	-7	32	
Rolandic operculum	L	4.952	-39	-28	20	
Superior temporal gyrus	L	4.370	-63	-34	14	
Supramarginal gyrus	L	4.874	-63	-25	29	
Inferior parietal gyrus, excluding supramarginal and angular gyri	R	3.731	48	-43	53	147
Postcentral gyrus	R	4.300	39	-37	59	
Precentral gyrus	R	4.780	27	-22	50	
Supplementary motor area	R	3.899	15	-19	62	
Insula	R	4.528	51	-4	2	125
Rolandic operculum	R	3.836	63	2	5	
Superior temporal gyrus	R	3.471	48	-1	-13	
Temporal pole: superior temporal gyrus	R	4.417	60	8	-1	
Superior frontal gyrus, dorsolateral	L	4.083	-12	65	17	110
Superior frontal gyrus, medial	L	5.419	0	65	20	
Superior frontal gyrus, medial	R	3.667	3	56	14	
Superior frontal gyrus, medial orbital	L	4.486	-6	44	-10	
Middle frontal gyrus	L	4.545	-33	35	32	90
Rolandic operculum	L	4.481	-54	-7	8	70
Superior temporal gyrus	L	5.002	-60	-1	2	
Insula	R	4.178	45	20	-10	58
Temporal pole: superior temporal gyrus	R	4.789	45	17	-22	
Precentral gyrus	R	4.001	30	-7	53	55
Superior frontal gyrus, dorsolateral	R	4.202	33	-4	62	
Middle temporal gyrus	R	4.147	66	-25	-7	53
Postcentral gyrus	R	4.570	63	-7	20	
Precentral gyrus	R	4.069	60	8	23	
Superior temporal gyrus	R	4.423	57	-22	-7	
Superior frontal gyrus, dorsolateral	R	4.331	24	50	41	52
Superior frontal gyrus, medial	R	4.538	12	50	47	

Note. Table shows one local maxima for each region within each cluster that is separated by more than 8mm. Regions are reported separately for each hemisphere and up to 50 peaks are reported per cluster. Regions were automatically labeled using the BSPMview (http://www.bobspunt.com/bspmview/) implementation of the AAL2 brain parcellation (Rolls, Joliot, & Tzourio-Mazoyer, 2015). Regions not identified by BSPMview (DOI 10.5281/zenodo.168074) with AAL2 were identified based on neuroanatomical examination with the BSPMview implementation of AAL Toolbox (Eickhoff et al., 2005); WFU Pickatlas Individual brain atlases using AAL (Tzourio-Mazoyer et al., 2002), IBASPM71 (Alemán-Gómez, Melie-García, & Valdés-Hernandez, 2006), Talairach Daemon (TD Labels, TD lobes, TD Brodmann areas+) (Lancaster, 1997; Lancster et al., 1997; Lancaster et al., 2000); Haines Neuroanatomy Atlas (Haines, 2012); and coordinate association in Neurosynth (http://www.neurosynth.org/) (Yarkoni, Poldrack, Nichols, Van Essen, & Wager, 2011). Local maxima are reported with Montreal Neurological Institute (MNI) coordinates x, y, and z in the left-right, anterior-posterior, and inferior-superior dimensions, respectively. Maximal Pseudo-T statistics, and extent in voxels (k) are reported for all significant clusters (cluster defining threshold = 3.01, cluster threshold FWE-corrected $p<0.05$; critical suprathreshold cluster size =37).

Table 10

Functional Connectivity for Positive Stimuli With Right Amygdala Seed Region

		Pseudo	MNI Coordinates			
Region Label	L/R	t-value	x	y	z	Extent
Calcarine fissure and surrounding cortex	L	5.799	-21	-64	5	3210
Calcarine fissure and surrounding cortex	R	5.019	18	-64	11	
Cerebellum crus I	R	4.324	39	-67	-31	
Cerebellum lobule IV, V	L	4.551	-6	-49	-1	
Cerebellum lobule VI	R	5.617	33	-61	-22	
Cuneus	R	4.663	12	-67	20	
Fusiform gyrus	L	4.907	-33	-70	-16	

Fusiform gyrus	R	6.530	27	-73	-16	
Inferior temporal gyrus	R	4.681	57	-67	-4	
Lingual gyrus	L	4.851	-12	-55	-1	
Lingual gyrus	R	4.399	15	-67	-10	
Middle occipital gyrus	L	5.362	-33	-82	2	
Middle occipital gyrus	R	4.283	30	-94	5	
Middle temporal gyrus	L	5.259	-51	-67	2	
Middle temporal gyrus	R	5.118	51	-64	5	
Paracentral lobule	L	6.010	0	-34	56	
Parahippocampal gyrus	R	4.376	27	-40	-4	
Postcentral gyrus	R	4.335	15	-37	68	
Precuneus	L	4.774	-24	-55	2	
Precuneus	R	6.442	9	-70	41	
Superior occipital gyrus	L	4.674	-18	-82	38	
Superior parietal lobule	R	4.808	15	-67	53	
Supplementary motor area	R	5.102	9	-25	50	
Amygdala	L	3.390	-30	-1	-13	615
Caudate nucleus	L	4.560	-12	11	-1	
Caudate nucleus	L	4.343	-12	-1	14	
Caudate nucleus	R	4.184	9	-1	8	
Heschl's gyrus	L	4.435	-30	-25	5	
Inferior frontal gyrus, pars opercularis	L	4.496	-54	8	14	
Inferior frontal gyrus, pars triangularis	L	3.942	-57	20	-7	
Insula	L	4.912	-36	-10	-4	
Lenticular nucleus, Pallidum	L	4.346	-24	-4	-1	
Lenticular nucleus, Putamen	L	5.532	-30	-13	2	
Postcentral gyrus	L	4.399	-51	-4	20	
Precentral gyrus	L	5.347	-54	5	29	
Superior temporal gyrus	L	4.348	-57	-1	-1	
Temporal pole: superior temporal gyrus	L	6.046	-48	11	-7	
Thalamus	L	4.643	0	-4	14	
Amygdala	R	9.674	24	-1	-16	589
Fusiform gyrus	R	4.731	39	-10	-34	
Heschl's gyrus	R	4.524	42	-19	11	
Hippocampus	R	4.988	21	-16	-16	
Inferior temporal gyrus	R	3.408	48	2	-37	
Insula	R	4.753	33	-22	17	
Lenticular nucleus, Putamen	R	4.471	30	-4	2	
Middle temporal gyrus	R	5.103	54	-31	-4	
Parahippocampal gyrus	R	4.046	21	-19	-25	
Rolandic operculum	R	3.953	63	-13	14	
Superior temporal gyrus	R	4.834	42	-16	-1	
Temporal pole: middle temporal gyrus	R	3.641	36	11	-37	
Thalamus	R	3.904	15	-10	-4	
Middle frontal gyrus	L	4.518	-42	53	20	119
Superior frontal gyrus, dorsolateral	L	5.136	-24	23	35	
Inferior frontal gyrus, pars opercularis	R	3.328	54	14	35	116
Inferior frontal gyrus, pars triangularis	R	3.716	54	23	5	
Middle frontal gyrus	R	4.270	39	11	44	
Precentral gyrus	R	4.668	51	5	44	116
Amygdala	L	4.511	-15	-4	-10	110
Hippocampus	L	4.769	-24	-16	-19	
Inferior parietal gyrus, excluding supramarginal and angular gyri	R	3.792	42	-55	50	97
Supramarginal gyrus	R	4.874	60	-31	32	

Caudate nucleus	R	4.998	18	17	-4	94
Inferior frontal gyrus, pars orbitalis	R	4.410	48	17	-10	
Insula	R	4.262	51	11	-4	
Temporal pole: superior temporal gyrus	R	4.451	57	20	-13	
Middle frontal gyrus	L	4.502	-30	11	47	67
Precentral gyrus	L	4.848	-27	-7	53	
Superior frontal gyrus, dorsolateral	L	3.608	-21	2	47	
Middle frontal gyrus	R	4.868	36	-1	62	66
Postcentral gyrus	R	3.943	60	-13	38	
Precentral gyrus	R	3.881	45	-4	50	
Postcentral gyrus	L	4.593	-60	-7	35	64
Supramarginal gyrus	L	4.261	-63	-25	29	
Thalamus	L	5.036	-9	-16	2	58
Inferior frontal gyrus, pars opercularis	R	4.349	48	11	17	56
Rolandic operculum	R	4.230	57	-1	5	
Middle cingulate & paracingulate gyri	R	3.586	9	2	38	53
Supplementary motor area	L	4.928	0	-4	56	
Supplementary motor area	R	3.952	6	-1	47	
Postcentral gyrus	R	4.496	30	-49	65	51
Superior parietal lobule	R	4.318	18	-46	68	
Superior frontal gyrus, medial	L	4.330	0	68	20	49
Superior frontal gyrus, medial	R	4.290	3	56	14	
Superior parietal lobule	L	4.279	-24	-55	56	
Lenticular nucleus, Putamen	R	4.303	24	-4	20	47
Thalamus	R	5.181	6	-19	5	
Inferior parietal gyrus, excluding supramarginal and angular gyri	R	3.184	51	-40	50	46
Postcentral gyrus	R	4.664	39	-34	53	
Postcentral gyrus	R	3.603	45	-37	62	
Supramarginal gyrus	L	4.225	-57	-40	35	
Anterior cingulate gyrus	R	3.820	9	41	20	43
Superior frontal gyrus, medial	L	4.040	3	35	35	
Posterior cingulate gyrus	L	4.745	-9	-37	23	38
Superior temporal gyrus	R	4.613	66	-40	11	37
Superior temporal gyrus	R	4.377	63	-31	17	
Middle frontal gyrus	R	4.337	42	50	5	36

Note. Table shows one local maxima for each region within each cluster that is separated by more than 8mm. Regions are reported separately for each hemisphere and up to 50 peaks are reported per cluster. Regions were automatically labeled using the BSPMview (http://www.bobspunt.com/bspmview/) implementation of the AAL2 brain parcellation (Rolls, Joliot, & Tzourio-Mazoyer, 2015). Regions not identified by BSPMview (DOI 10.5281/zenodo.168074) with AAL2 were identified based on neuroanatomical examination with the BSPMview implementation of AAL Toolbox (Eickhoff et al., 2005); WFU Pickatlas Individual brain atlases using AAL (Tzourio-Mazoyer et al., 2002), IBASPM71 (Alemán-Gómez, Melie-García, & Valdés-Hernandez, 2006), Talairach Daemon (TD Labels, TD lobes, TD Brodmann areas+) (Lancaster, 1997; Lancaster et al., 1997; Lancaster et al., 2000); Haines Neuroanatomy Atlas (Haines, 2012); and coordinate association in Neurosynth (http://www.neurosynth.org/) (Yarkoni, Poldrack, Nichols, Van Essen, & Wager, 2011). Local maxima are reported with Montreal Neurological Institute (MNI) coordinates x, y, and z in the left-right, anterior-posterior, and inferior-superior dimensions, respectively. Maximal Pseudo-T statistics, and extent in voxels (k) are reported for all significant clusters (cluster defining threshold = 3.01, cluster threshold FWE-corrected $p<0.05$; critical suprathreshold cluster size =43).

Table 11

Small Volume Correction Regional Activations and Functional Connectivity

					MNI Coordinates		
Contrast Name	Region Label	L/R	Extent	Pseudo t-value	x	y	z
Emotion>Neutral	Amygdala	R	20	5.43	18	-1	-16
Emotion>Neutral	Amygdala	L	21	5.09	-18	-4	-16
Positive>Neutral	Amygdala	L	20	5.11	-18	-7	-16
Positive>Neutral	Amygdala	R	11	4.23	21	-1	-19
Negative>Neutral	Amygdala	R	18	5.27	18	-1	-16
Negative>Neutral	Amygdala	L	18	4.66	-21	-1	-16
DM	Hippocampus	L	14	4.28	-27	-25	-13
DM	Hippocampus	L	14	3.63	-33	-22	-19
PositiveDM	Hippocampus	L	9	3.87	-24	-22	-13
PositiveDM	Hippocampus	L	9	3.47	-24	-28	-7
NegativeDM	Hippocampus	no activation clusters					
EmotionDM	Hippocampus	no activation clusters					
NeutralDM	Hippocampus	no activation clusters					
EmotionDM>NeutralDM	Hippocampus	no activation clusters					
NegativeDM>NeutralDM	Hippocampus	no activation clusters					
PositiveDM>NeutralDM	Hippocampus	no activation clusters					
PositiveDM	Amygdala	no activation clusters					
NegativeDM	Amygdala	no activation clusters					
EmotionDM	Amygdala	no activation clusters					
NeutralDM	Amygdala	no activation clusters					
EmotionDM>NeutralDM	Amygdala	no activation clusters					
NegativeDM>NeutralDM	Amygdala	no activation clusters					
PositiveDM>NeutralDM	Amygdala	no activation clusters					

Note. Table shows all local maxima separated by more than 8 mm. Regions were automatically labeled using the AAL2 atlas. x, y, and z =Montreal Neurological Institute (MNI) coordinates in the left-right, anterior-posterior, and inferior-superior dimensions, respectively. Maximal Pseudo-T statistics, and extent in voxels (k) are reported for all significant clusters (cluster defining threshold = 3.01, cluster threshold FWE-corrected $p<0.05$; critical suprathreshold cluster size =4 for DM contrast; critical suprathreshold cluster size = 4 for Positive DM contrast)